

Charge regulation and local dielectric function in planar polyelectrolyte brushes

Rajeev Kumar *

*National Center for Computational Sciences,
Oak Ridge National Laboratory, Oak Ridge, TN-37831*

Bobby G. Sumpter

*Center for Nanophase Materials Sciences,
Oak Ridge National Laboratory, Oak Ridge, TN-37831*

S. Michael Kilbey II

*Center for Nanophase Materials Sciences,
Oak Ridge National Laboratory,
Oak Ridge, TN-37831*

&

*Department of Chemistry,
University of Tennessee,
Knoxville, TN-37996*

(Dated: March 8, 2013)

Understanding the effect of inhomogeneity on the charge regulation and dielectric properties, and how it depends on the conformational characteristics of the macromolecules is a long-standing problem. In order to address this problem, we have developed a field-theory to study charge regulation and *local* dielectric function in planar polyelectrolyte brushes. The theory is used to study a polyacid brush, which is comprised of chains end-grafted at the solid-fluid interface, in equilibrium with a bulk solution containing monovalent salt ions, solvent molecules and pH controlling acid. In particular, we focus on the effects of the concentration of added salt and pH of the bulk in determining the local charge and dielectric function. Our theoretical investigations reveal that the dipole moment of the ion-pairs formed as a result of

* To whom any correspondence should be addressed, Email : kumarr@ornl.gov

counterion adsorption on the chain backbones play a key role in affecting the local dielectric function. For polyelectrolytes made of monomers having dipole moments lower than the solvent molecules, dielectric decrement is predicted inside the brush region. However, the formation of ion-pairs (due to adsorption of counterions coming from the dissociation of added salt) more polar than the solvent molecules is shown to increase the magnitude of the dielectric function with respect to its bulk value. Furthermore, an increase in the bulk salt concentration is shown to increase the local charge inside the brush region.

I. INTRODUCTION

Polyelectrolyte brushes[1–6] have been used extensively in the development of stimuli-sensitive materials due to their ultra-sensitive response to different stimuli such as pH, temperature, solvent etc. A fundamental understanding of the effect of each of these stimuli on the brush properties is highly desirable for a number of technologies. Extensive research[7–22] aimed at elucidating the effect of different experimental variables on the response of polyelectrolyte brushes has been conducted. However, in general, dielectric properties of polyelectrolytes[23–27] elude a clear understanding and are rarely studied using rigorous theoretical tools.

Classic literature on the dielectric function[28–33] mainly deals with the small molecules randomly distributed in space, constituting a spatially homogeneous medium. For a spatially uniform medium, in the absence of explicit charges, the dielectric function also turns out to be invariant in space and hence, the words “dielectric constant” are used in place of “dielectric function”. For a single charge in a polar medium, it has been shown[28–36] that the dielectric function depends on the distance from the charge. The dielectric function is lowest next to the charge and monotonically approaches the dielectric constant of the medium. This effect is known as the dielectric saturation effect[28] resulting from the strong electric field next to the charge, which vanishes with an increase in the distance from the charge, reaching zero in the bulk.

The dielectric saturation effect has been shown[28] to be responsible for the dielectric decrement when *trace* amounts of electrolytes like sodium chloride are added to polar solvents such as water. In particular, a linear dependence of the dielectric decrement on the

salt concentration was proposed by Debye[28]. The linear relation between the dielectric decrement and the salt concentration was also observed in experiments[28]. However, the situation at large concentrations of salt is far more complex due to the interplay between association/ion-pairing and short-range interactions.

Like electrolytes, polyelectrolytic systems are inherently inhomogeneous. Understanding the effect of inhomogeneity on the dielectric properties of the macromolecules is a long-standing problem. To the best of our knowledge, there is no comprehensive theory for the *local* dielectric function of polyelectrolytes, despite a large body of experimental work[23–26], which has shown that addition of polyelectrolytes to a solution containing polar solvent and salt leads to dielectric increment[23–26]. Minakata et al.[27] attributed the *overall* dielectric increment to the fluctuations of the bound counterion charge at different sites. However, the theory by Minakata et al.[27] ignores the conformational degrees of freedom and deals with *rod-like* polyelectrolytes in an external electric field.

From the above discussion, it is clear that the dielectric function depends on the number of charges and their distribution. This dependence of the dielectric function adds another complexity in the case of polyelectrolytes. The complexity arises because of the tendency of polyelectrolytes to regulate their charges[37–41] on the basis of the local environment such as local pH, salt concentration, etc. In other words, one has to compute the local charge and the dielectric function in a self-consistent manner while minimizing the free energy. In this work, we have developed a quantitative description of the charge regulation and local dielectric function for polyelectrolytes. The theoretical formalism is quite general and we use it to study a planar polyelectrolyte brush in equilibrium with a solution bath containing monovalent salt ions, solvent molecules and an acid to control the pH of the bath. This particular set-up serves as a model system and is relevant for a number of experimental studies. Typically, solvent molecules are treated as a continuum without having any structure. Here, we treat each solvent molecule as having a permanent dipole moment of its own, which is a reasonable model representation of a number of polar molecules. For a quantitative analysis of the dielectric function, which must depend on the local properties such as density, electrostatic potential and electric field, we have developed a field-theory taking into account the dipolar interactions between charged and uncharged components.

This paper is organized as follows: the general formalism is presented in section II and details about the application of the formalism to the polyelectrolyte brushes are presented

in section III. Numerical results are presented in section IV, and section V contains our conclusions.

II. THEORY

We consider a planar polyelectrolyte brush formed by n mono-disperse flexible polyacid chains (such as poly(methacrylic acid)), each having N Kuhn segments of length l . The chains are assumed to be uniformly grafted onto an uncharged substrate so that the grafting density (defined as the number of chains per square nanometer) is σ (see Fig. 1). For the field theoretical analysis[42, 43] described in this work, each polyelectrolyte chain is represented by a continuous curve of length Nl , and an arc variable t is used to represent any segment along the backbone so that $t \in [0, N]$. $t = 0$ corresponds to the grafted end and $t = N$ represents the other end. To keep track of different grafted chains, subscript α is used so that t_α represents the contour variable along the backbone of α^{th} chain. In the following, we use the notation $\mathbf{R}_\alpha(t_\alpha)$ to represent the position vector for a particular segment, t_α , along the α^{th} chain.

Counterion adsorption on the chains is studied using a two-state model. In this model, the entire population of counterions is divided based on whether they are “free” or “adsorbed”. As the label implies, the “free” counterions are free to sample the whole space, while the “adsorbed” counterions have less translational degrees of freedom and are bound to the chains. In other words, each segment of a chain can be in either uncharged or charged state. The adsorbed counterions/uncharged segments are treated as “point” dipoles. For each uncharged segment t_α along the α^{th} chain, an electric dipole of moment (in units of electronic charge, e) $\mathbf{p}_\alpha(t_\alpha)$ is assigned. Similarly, each solvent molecule is assigned an electric dipole moment and we use the notation \mathbf{p}_k to represent the dipole moment of the k^{th} solvent molecule. Interactions between the charged and uncharged species are taken into account by ion-dipole potentials.

In this work, we focus on the effects of “permanent dipole moments” and don’t allow variations in the magnitude of the electric dipole moments. However, we allow the dipoles to be aligned depending on the local electric field. The physical origin of these electric dipoles is the difference in electronegativities of the atoms constituting the dissociable group along the backbone. For example, acetic acid has a dipole moment of 1.7 Debye[44]. It is well-

known[28–31] that finite polarizability of molecules leads to an enhancement of net electric dipole moments. We plan to include these effects in future work.

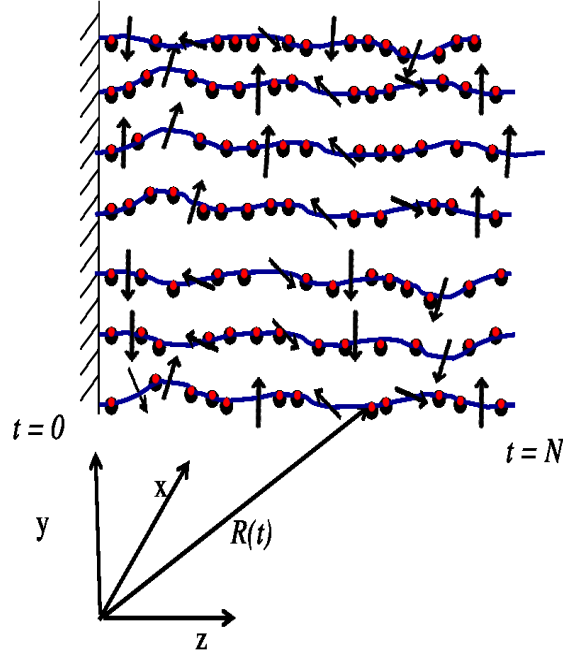


FIG. 1: Schematic of a planar polyelectrolyte brush containing monodisperse chains in equilibrium with an electrolyte solution (not shown explicitly here). The polyelectrolyte chains are modeled as continuous curves containing charges (represented by red dots) and electric dipoles (represented by arrows) resulting from counterion adsorption. The pH regulating electrolyte solution is assumed to contain two kinds of counterions resulting into two kinds of dipoles on the chains.

We assume that the brush is in equilibrium with a bulk solution whose pH is controlled by the use of a buffer containing an acid and the precise concentrations of protons, H^+ , cations from the added salt, B^+ , and anions, A^- , which result from the dissociation of the acid, water molecules (protons and hydroxyl ions) and the salt, are known. For the sake of simplicity, we assume that the anions coming from the acid, water molecules and the salt are indistinguishable. Generalization of the theory presented here to take into account the specificity of anions is straightforward. However, we consider the specificity of cations (counterions for the brush) to study the effects of dipole moments of different kinds of ion-pairs and competitive counterion adsorption. Physically, H^+ originates from the dissociation of acidic sites on the polyelectrolytes, protonation of water molecules and the acid (for pH

< 7). In this paper, we use the word “bulk” quite frequently while referring to the region in space, where electrostatic potential and densities are spatially independent. One should not confuse the region just outside the brush region as the “bulk”, because the electrostatic potential may be inhomogeneous even in monomer-free regions.

The theory is developed in the Canonical ensemble and the equilibrium with the bulk solution is considered by equating the chemical potentials of different components in the inhomogeneous brush and the homogeneous bulk solution. For the theoretical treatment carried out in the Canonical ensemble, we assume that there are n_γ ions of kind $\gamma = H^+, B^+, A^-$. The number of counterions in the “free” and “adsorbed” states are represented by superscripts f and a , respectively. Overall, the system is electroneutral and local electroneutrality is assumed for the bulk solution. To keep track of different kinds of ions, we define Z_γ as the valency (with sign) of the charged species $\gamma = H^+, B^+, A^-, p$, where the subscript p represents the polymers. For monovalent ions, $|Z_\gamma| = 1$ and for a polyacid, $Z_p = -1$.

Following the mathematical procedure presented in Appendices A and B, we can write the partition function for the polyelectrolyte brushes as

$$Z = \frac{1}{\Xi} \int D[\rho_p] \int D[w_p] \int D[w_s] \int D[\psi] \exp \left[-\frac{F_0}{k_B T} - \frac{H}{k_B T} \right] \quad (1)$$

where

$$\frac{F_0}{k_B T} = \frac{F_a}{k_B T} + \frac{1}{2} [w_{pp}\rho_{po}nN + w_{ss}\rho_{so}n_s] - \ln \left[\Omega \sum_{\gamma'} n_{\gamma'}^f + n_{A^-} + n_s \right], \quad \gamma' = H^+, B^+ \quad (2)$$

and F_a contains contributions coming from the adsorbed counterions. Explicitly, it is given by (see Appendix B)

$$\begin{aligned} \frac{F_a}{k_B T} = & n_{B^+}^a \ln K_{B^+} - (nN - n_{H^+}^a) \ln K_{H^+} - \ln \left[\frac{nN!}{n_{H^+}^a! n_{B^+}^a! (nN - n_{H^+}^a - n_{B^+}^a)!} \right] \\ & + \ln [n_{H^+}^f! n_{B^+}^f! n_s!] - (nN + n_s) \ln 4\pi \end{aligned} \quad (3)$$

In writing Eq. 3, we have defined an equilibrium constant, K_{H^+} , for the dissociation of acidic groups on the polyelectrolyte chains by the thermodynamic relation[45] $K_{H^+} = \exp[-\{\mu_{COO^-}^o + \mu_{H^+}^o - \mu_{COOH}^o\}]$ where μ is the chemical potential (in units of $k_B T$, the Boltzmann constant times the absolute temperature) and superscript o represents the limit of infinite dilution. Similarly, we have defined another equilibrium constant K_{B^+} for the binding of the counterions from the salt by the relation $K_{B^+} = \exp[-\{\mu_{COO^-}^o + \mu_{B^+}^o - \mu_{COO^- B^+}^o\}]$.

Also,

$$\begin{aligned} \frac{H}{k_B T} = & \chi_{ps} \int d\mathbf{r} \rho_p(\mathbf{r}) \rho_{so} \left[1 - \frac{\rho_p(\mathbf{r})}{\rho_{po}} \right] + i \int d\mathbf{r} [\psi_p(\mathbf{r}) - w_p(\mathbf{r})] \rho_p(\mathbf{r}) \\ & - \frac{1}{8\pi l_{Bo}} \int d\mathbf{r} \psi(\mathbf{r}) \nabla_{\mathbf{r}}^2 \psi(\mathbf{r}) - i \int d\mathbf{r} \rho_{so} \left[1 - \frac{\rho_p(\mathbf{r})}{\rho_{po}} \right] \left[w_s(\mathbf{r}) + \ln \left[\frac{\sin(p_s |\nabla_{\mathbf{r}} \psi(\mathbf{r})|)}{p_s |\nabla_{\mathbf{r}} \psi(\mathbf{r})|} \right] \right] \\ & - \sum_{\gamma'=H^+, B^+} n_{\gamma'}^f \ln Q_{\gamma'} \{\psi\} - n_{A^-} \ln Q_{A^-} \{\psi\} - n_s \ln Q_s \{w_s\} - \sum_{\alpha=1}^n Q_{p\alpha} \{w_p\} \end{aligned} \quad (4)$$

Here, Q_{γ} , Q_s and $Q_{p\alpha}$ are the *normalized* partition functions for a small ion of type γ , solvent molecule, and α^{th} grafted chain, respectively, given by

$$Q_{\gamma} \{\psi\} = \frac{1}{\Omega} \int d\mathbf{r} \exp[-iZ_{\gamma}\psi(\mathbf{r})] \quad \text{for } \gamma = H^+, B^+, A^- \quad (5)$$

$$Q_s \{w_s\} = \frac{1}{\Omega} \int d\mathbf{r} \exp[-iw_s(\mathbf{r})] \quad (6)$$

and

$$Q_{p\alpha} \{w_p\} = \int_{\mathbf{R}_{\alpha}(0)=\mathbf{r}_{\alpha}} D[\mathbf{R}_{\alpha}(t_{\alpha})] \exp \left[-\frac{3}{2l^2} \int_0^N dt_{\alpha} \left(\frac{\partial \mathbf{R}_{\alpha}(t_{\alpha})}{\partial t_{\alpha}} \right)^2 - i \int_0^N dt_{\alpha} w_p(\mathbf{R}_{\alpha}) \right] \quad (7)$$

where \mathbf{r}_{α} is the position vector for the grafted end of the α^{th} chain.

In these equations, $\psi(\mathbf{r})$ is the collective field introduced to decouple electrostatic interactions and it is the equivalent to the electrostatic potential. $w_p(\mathbf{r})$, $w_s(\mathbf{r})$ are the fields introduced to decouple short range interactions modeled by the Edwards' delta functional approach[42, 43]. $\rho_p(\mathbf{r})$ is the collective density variable. The Edwards' approach for using a delta function potential to model short range interactions along with the local incompressibility constraint naturally leads to appearance of the parameter χ_{ps} in the theory, defined in terms of excluded volume parameters w_{pp} , w_{ss} and w_{ps} in Appendix B.

Also, $l_{Bo} = e^2/\epsilon_o k_B T$ is the Bjerrum length in vacuum, where e is the charge on an electron and ϵ_o being the permittivity of vacuum. Ω is the total volume of the system and $p_s = |\mathbf{p}_k|$ is the magnitude of the dipole moment of each solvent molecule. ρ_{po} and ρ_{so} are the densities of pure polymers and solvent, respectively, and Ξ is a normalizing factor defined in the Appendix B. The function ψ_p appearing in Eq. 4 is given by (see Appendix B)

$$\exp[-i\psi_p(\mathbf{r})] = (1 - \beta_{H^+} - \beta_{B^+}) \exp[-iZ_p\psi(\mathbf{r})] + \sum_{\gamma'=H^+, B^+} \beta_{\gamma'} \left[\frac{\sin(p_{\gamma'} |\nabla_{\mathbf{r}} \psi(\mathbf{r})|)}{p_{\gamma'} |\nabla_{\mathbf{r}} \psi(\mathbf{r})|} \right] \quad (8)$$

where $\beta_{\gamma'}, \gamma' = H^+, B^+$ are the variational parameters characterizing the extent of counterion adsorption of type γ' on the polyelectrolyte chains. These parameters need to be determined by the minimization of the free energy of the system. Furthermore, $p_{\gamma'}$ is the magnitude of the dipole moment of an ion-pair formed by the adsorption of counterion of type γ' .

In the next section, we present the implications of the dipolar interactions on the properties of planar polyelectrolyte brushes in equilibrium with a solution containing monovalent salt.

III. PLANAR POLYELECTROLYTE BRUSH IN EQUILIBRIUM WITH A SOLUTION BATH

A. Saddle-point approximation

An inhomogenous polyelectrolyte brush in equilibrium with a salty solution can be studied using the saddle-point approximation[43]. The approximation evaluates the functional integrals over the fields by the value of the integrand at the saddle-point. Optimizing the Hamiltonian given by Eq. 4 with respect to w_p, w_s, ρ_p and ψ , respectively, we obtain

$$\rho_p^*(\mathbf{r}) = - \sum_{\alpha=1}^n \frac{\delta \ln Q_{p\alpha} \{w_p^*\}}{\delta w_p^*(\mathbf{r})} \quad (9)$$

$$\rho_{so} \left[1 - \frac{\rho_p^*(\mathbf{r})}{\rho_{po}} \right] = \frac{n_s \exp[-w_s^*(\mathbf{r})]}{\int d\mathbf{r} \exp[-w_s^*(\mathbf{r})]} \quad (10)$$

$$w_p^*(\mathbf{r}) = \psi_p^*(\mathbf{r}) + \frac{\rho_{so}}{\rho_{po}} \left\{ w_s^*(\mathbf{r}) + \ln \left[\frac{\sinh(p_s |\nabla_{\mathbf{r}} \psi^*(\mathbf{r})|)}{p_s |\nabla_{\mathbf{r}} \psi^*(\mathbf{r})|} \right] \right\} + \chi_{ps} \rho_{so} \left[1 - \frac{2\rho_p^*(\mathbf{r})}{\rho_{po}} \right] \quad (11)$$

$$\nabla_{\mathbf{r}} \cdot \left[\frac{1}{l_B \{\rho_p^*, \psi^*\}} \nabla_{\mathbf{r}} \psi^*(\mathbf{r}) \right] = -4\pi \left[\sum_{\gamma'=H^+, B^+} Z_{\gamma'} \rho_{\gamma'}^*(\mathbf{r}) + Z_{A^-} \rho_{A^-}^*(\mathbf{r}) + Z_p \beta^*(\mathbf{r}) \rho_p^*(\mathbf{r}) \right] \quad (12)$$

Here, we have used the notation $iw_p(\mathbf{r}) = w_p^*(\mathbf{r})$, $iw_s(\mathbf{r}) = w_s^*(\mathbf{r})$, $i\psi(\mathbf{r}) = \psi^*(\mathbf{r})$, $i\psi_p(\mathbf{r}) = \psi_p^*(\mathbf{r})$ because the collective fields are purely imaginary[43] at the saddle point. Also, the collective density variables such as $\rho_p(\mathbf{r})$ at the saddle point are as $\rho_p^*(\mathbf{r})$. $\rho_{\gamma}^*(\mathbf{r})$ in Eq. 12 is the number density of small ions of type $\gamma = H^+, B^+, A^-$, given by

$$\rho_{\gamma}^*(\mathbf{r}) = \frac{n_{\gamma} \exp[-Z_{\gamma} \psi^*(\mathbf{r})]}{\int d\mathbf{r} \exp[-Z_{\gamma} \psi^*(\mathbf{r})]} \quad (13)$$

where $n_\gamma = n_\gamma^f$ for $\gamma = H^+, B^+$. In other words, only the “free” counterions appear in Eq. 12. Furthermore, the effective Bjerrum length in Eq. 12 is given by

$$\frac{1}{l_B \{\rho_p^*, \psi^*\}} = \frac{1}{l_{Bo}} + 4\pi \left\{ \sum_{\gamma'=H^+, B^+} p_{\gamma'}^2 p_{\gamma'}^*(\mathbf{r}) \rho_p^*(\mathbf{r}) \bar{L} [p_{\gamma'} |\nabla_{\mathbf{r}} \psi^*(\mathbf{r})|] \right. \\ \left. + p_s^2 \rho_{so} \left[1 - \frac{\rho_p^*(\mathbf{r})}{\rho_{po}} \right] \bar{L} [p_s |\nabla_{\mathbf{r}} \psi^*(\mathbf{r})|] \right\} \quad (14)$$

where $\bar{L}(x) = L(x)/x$ so that $L(x) = \coth x - 1/x$ is the Langevin function. Furthermore,

$$\beta^*(\mathbf{r}) = \frac{(1 - \beta_{H^+} - \beta_{B^+}) \exp [-Z_p \psi^*(\mathbf{r})]}{\exp [-\psi_p^*(\mathbf{r})]} \quad (15)$$

$$p_{\gamma'}^*(\mathbf{r}) = \frac{\beta_{\gamma'}}{\exp [-\psi_p^*(\mathbf{r})]} \frac{\sinh(p_{\gamma'} |\nabla_{\mathbf{r}} \psi^*(\mathbf{r})|)}{p_{\gamma'} |\nabla_{\mathbf{r}} \psi^*(\mathbf{r})|} \quad (16)$$

so that ψ_p^* is given by Eq. 8 at the saddle point with the notation $i\psi_p(\mathbf{r}) = \psi_p^*(\mathbf{r})$. Explicitly, it is given by

$$\exp [-\psi_p^*(\mathbf{r})] = (1 - \beta_{H^+} - \beta_{B^+}) \exp [-Z_p \psi^*(\mathbf{r})] + \sum_{\gamma'=H^+, B^+} \beta_{\gamma'} \left[\frac{\sinh(p_{\gamma'} |\nabla_{\mathbf{r}} \psi^*(\mathbf{r})|)}{p_{\gamma'} |\nabla_{\mathbf{r}} \psi^*(\mathbf{r})|} \right] \quad (17)$$

Note that $\beta^*(\mathbf{r}) + \sum_{\gamma'=H^+, B^+} p_{\gamma'}^*(\mathbf{r}) = 1$. From Eqs. 15 and 16 we can interpret that $\beta^*(\mathbf{r})$ and $p_{\gamma'}^*(\mathbf{r})$ denote the probability of finding a charge and a dipole resulting from adsorption of counterion of type γ , respectively, at location \mathbf{r} .

Invoking the relation between the Bjerrum length and local dielectric function, $l_B \{\rho_p^*, \psi^*\} = e^2/\epsilon \{\rho_p^*, \psi^*\} k_B T$, we obtain

$$\frac{\epsilon \{\rho_p^*, \psi^*\}}{\epsilon_o} = 1 + 4\pi l_{Bo} \left[\sum_{\gamma'=H^+, B^+} p_{\gamma'}^2 p_{\gamma'}^*(\mathbf{r}) \rho_p^*(\mathbf{r}) \bar{L} [p_{\gamma'} |\nabla_{\mathbf{r}} \psi^*(\mathbf{r})|] \right. \\ \left. + p_s^2 \rho_{so} \left[1 - \frac{\rho_p^*(\mathbf{r})}{\rho_{po}} \right] \bar{L} [p_s |\nabla_{\mathbf{r}} \psi^*(\mathbf{r})|] \right] \quad (18)$$

It is worth noting that the functional form of the field dependent dielectric function in Eq. 18 is qualitatively similar to the expression derived in the classic papers by Onsager[29] and Booth[31, 32]. Noting that $\bar{L}(x)$ decreases with an increase in x and $\sinh x/x$ (appearing in $p_{\gamma'}^*$, cf. Eq. 16) increases with an increase in x , the local field can lead to dielectric decrement or increment depending on the relative strength of these counteracting effects. In other words, the first effect (also arising in the Langevin-Debye model[28] and known as the dielectric saturation effect) tends to lower the dielectric function. On the other hand, the second effect resulting from the counterion adsorption tend to increase it.

An important insight into the effect of electric dipoles on the thermodynamics of the polyelectrolyte brushes is obtained if one considers the weak coupling limit for the electric dipoles (i.e., the limit of weak dipoles or weak local electric fields) so that $p_{\gamma'}|\nabla_{\mathbf{r}}\psi^*(\mathbf{r})| \rightarrow 0$, $p_s|\nabla_{\mathbf{r}}\psi^*(\mathbf{r})| \rightarrow 0$. In these limits we can either use the approximation $\ln[\sin x/x] \simeq -x^2/6$ in the expression for the partition function or $L(x) \rightarrow x/3$ for $x \rightarrow 0$ in Eq. 14. Using either of the approximations, it can be shown that the electric dipoles renormalize the Bjerrum length of the medium by the relation

$$\frac{1}{l_B\{\rho_p^*, \psi^*\}} \equiv \frac{1}{l_B\{\rho_p^*\}} = \frac{1}{l_{Bo}} + \frac{4\pi}{3} \left[\sum_{\gamma'=H^+, B^+} (p_{\gamma'}^2 \beta_{\gamma'}) \rho_p^*(\mathbf{r}) + p_s^2 \rho_{so} \left[1 - \frac{\rho_p^*(\mathbf{r})}{\rho_{po}} \right] \right] \quad (19)$$

This allows us to write $\epsilon(\mathbf{r}) = \epsilon_p \phi_p(\mathbf{r}) + \epsilon_s \phi_s(\mathbf{r})$, where $\phi_p(\mathbf{r}) = \rho_p^*(\mathbf{r})/\rho_{po}$ and $\phi_s(\mathbf{r}) = 1 - \rho_p^*(\mathbf{r})/\rho_{po}$ are the volume fractions of the monomers and solvent molecules, respectively. Also, ϵ_p and ϵ_s are the dielectric constants of the pure components, given by $\epsilon_p/\epsilon_o - 1 = 4\pi l_{Bo} \sum_{\gamma'=H^+, B^+} (\beta_{\gamma'} p_{\gamma'}^2) \rho_{po}/3$ and by $\epsilon_s/\epsilon_o - 1 = 4\pi l_{Bo} p_s^2 \rho_{so}/3$. In other words, the linear mixing rule based on the volume fractions can be used to estimate the local dielectric function of the medium in the weak-coupling limit.

Furthermore, by optimizing the Hamiltonian given by Eq. 4 with respect to the variational parameter β_{H^+} , we obtain

$$\begin{aligned} \log_{10} \left[\frac{\beta_{H^+}}{1 - \sum_{\gamma'} \beta_{\gamma'}} \frac{\int d\mathbf{r} \exp[-Z_{H^+} \psi^*(\mathbf{r})]}{n_{H^+}^f} \right] - \text{pK}_{H^+} \\ + \frac{1}{2.303nN} \int d\mathbf{r} \rho_p^*(\mathbf{r}) \left[\frac{\beta^*(\mathbf{r})}{1 - \sum_{\gamma'} \beta_{\gamma'}} - \frac{p_{H^+}^*(\mathbf{r})}{\beta_{H^+}} \right] = 0 \end{aligned} \quad (20)$$

where $\gamma' = H^+, B^+$. In deriving Eq. 20, we have used the fact that $n_{H^+}^f = n_{H^+}^{\text{total}} - \beta_{H^+} nN$. Also, we have defined $\text{pK}_{H^+} = -\log_{10} K_{H^+}$. The last term in Eq. 20 captures the effects of finite monomer density and inhomogeneity on the charge regulation in the brushes. This term can be interpreted as the shift in pK_{H^+} and depends on the local environment. However, sign of the shift depends on the relative contributions of the charges and dipole.

A similar equation is obtained for β_{B^+} , which can be written by replacing H^+ by B^+ in Eq. 20. For the binding of the counterions from the salt, we define $\text{pK}_{B^+} = -\log_{10} K_{B^+}$. Eq. 20 equates the chemical potentials of the counterions in the “free” state and the “adsorbed” state. In the next section, we present the details about the treatment of grafted ends in the theory.

B. Treatment of grafted ends: uniformly grafted brush

The functional derivative of the chain partition function with an end grafted at $\mathbf{R}_\alpha(0) = \mathbf{r}_\alpha$ on the substrate allows us to write Eq. 9 as

$$\rho_p^*(\mathbf{r}) = \sum_{\alpha=1}^n \frac{\int_0^N dt q_{\mathbf{r}_\alpha}(\mathbf{r}, t) \bar{q}(\mathbf{r}, N - t)}{\int d\mathbf{r} q_{\mathbf{r}_\alpha}(\mathbf{r}, t) \bar{q}(\mathbf{r}, N - t)}, \quad (21)$$

where $\bar{q}(\mathbf{r}, N - t)$ satisfies

$$\frac{\partial \bar{q}(\mathbf{r}, t')}{\partial t'} = \left[\frac{l^2}{6} \nabla_{\mathbf{r}}^2 - w_p^*(\mathbf{r}) \right] \bar{q}(\mathbf{r}, t') \quad (22)$$

with the condition $\bar{q}(\mathbf{r}, 0) = 1$ for $t' = N - t = 0$. Similarly, $q_{\mathbf{r}_\alpha}(\mathbf{r}, t)$ satisfies the same equation but with the initial condition $q_{\mathbf{r}_\alpha}(\mathbf{r}, 0) = \delta(\mathbf{r} - \mathbf{r}_\alpha)$.

Noting that the denominator in Eq. 21 is independent of t , Muller[46] has developed an efficient algorithm to solve these equations in three dimensional space. Following Muller, we choose $t = 0$ for the denominator in Eq. 21 and use the initial conditions for q and \bar{q} to write Eq. 21 as

$$\rho_p^*(\mathbf{r}) = \int_0^N dt \hat{q}(\mathbf{r}, t) \bar{q}(\mathbf{r}, N - t) \quad (23)$$

where

$$\hat{q}(\mathbf{r}, t) = \sum_{\alpha=1}^n \frac{q_{\mathbf{r}_\alpha}(\mathbf{r}, t)}{\bar{q}(\mathbf{r}_\alpha, N)} \simeq \sigma \int d\mathbf{r}_{2d} \frac{q_{\mathbf{r}_\alpha}(\mathbf{r}, t)}{\bar{q}(\mathbf{r}_\alpha, N)} \quad (24)$$

Here, $\int d\mathbf{r}_{2d}$ is the integral over the grafting points. The later transformation to go from a discrete sum over all the chains to the quadrature over the grafting points is strictly valid in the thermodynamic limit so that $n \rightarrow \infty$, A (=area of the grafting plane) $\rightarrow \infty$ and $\sigma = n/A$ is finite. Due to the linear relation between \hat{q} and $q_{\mathbf{r}_\alpha}$, \hat{q} also satisfies Eq. 22, but with the initial condition

$$\hat{q}(\mathbf{r}, 0) = \frac{\sigma \delta(z - \delta)}{\bar{q}(\{x, y, \delta\}, N)} \quad (25)$$

where we have written $\mathbf{r}_\alpha = \{x_\alpha, y_\alpha, \delta\}$ in Cartesian co-ordinates so that $\delta \rightarrow 0$ is the parameter used to put the anchoring point at an infinitesimal distance above the substrate.

The above transformation also allows us to write the sum over the chain partition functions in the Hamiltonian (cf. Eq. 4) in a manageable form, given by

$$\sum_{\alpha=1}^n \ln Q_{p\alpha} \{w_p\} \simeq \sigma \int d\mathbf{r}_{2d} \ln [\bar{q}(\{\mathbf{r}_{2d}, \delta\}, N)] \quad (26)$$

$$= \sigma A \ln [\bar{q}(\delta, N)] \quad (27)$$

The last expression is valid in the special case when $\bar{q}(\mathbf{r}, N)$ is a function of the distance from the substrate i.e., in the absence of lateral inhomogeneities. We call this particular case the one-dimensional brush because the densities of different components are dependent only on the distance from the substrate. This is the case for high grafting densities in good solvents.

C. Free energy with respect to the salty solution

For a polyelectrolyte brush in equilibrium with a solution containing monovalent salt, we have to equate the chemical potentials of all the components that can be exchanged between the bulk solution and the brush region. Also, at equilibrium, the osmotic pressure must be the same everywhere. However, due to the incompressibility constraint, equating the chemical potentials of the salt ions and solvent molecules is sufficient to define the equilibrium state of the system. Furthermore, it is assumed that the densities of different components are known in the bulk solution and we use them as parameters in the study here.

Using the thermodynamic relation between the free energy and chemical potentials in the canonical ensemble (i.e., $\mu_j = (\partial F / \partial n_j)_{\Omega, T}$), we get

$$\mu_\gamma = \ln \left[\frac{n_\gamma}{\int d\mathbf{r} \exp[-Z_\gamma \psi^*(\mathbf{r})]} \right] = \ln \rho_\gamma(\infty) + Z_\gamma \psi^*(\infty) \quad (28)$$

for the “free” ions, $\gamma = H^+, B^+, A^-$ so that $n_\gamma = n_\gamma^f$ for $\gamma = H^+, B^+$. In writing the second equation on the right in Eq. 28, we have used Eq. 13 and the boundary condition that the density of the “free” ions is given by $\rho_\gamma(\infty)$ in the bulk (designated by $\mathbf{r} \rightarrow \infty$). Also, $\psi^*(\infty)$ is the value of $\psi^*(\mathbf{r})$ in the bulk. The values of $\beta_{\gamma'}$ are determined by using Eq. 28 along with Eq. 20. An important insight into the effect of salt concentration on the charge regulation can be obtained by taking the limit of $\rho_p^*(\mathbf{r}) = 0$ (i.e., the limit of vanishing grafting density) in Eq. 20. Taking the limit of zero monomer density in Eq. 20 and using Eq. 28, we can write

$$\beta_{H^+} = \frac{1}{1 + 10^{\text{pH} - \text{pK}_{H^+}} \left[e^{-Z_+ \psi^*(\infty)/2.303} + \rho_{B^+}(\infty) 10^{\text{pK}_{B^+}} \right]} \quad (29)$$

$$\frac{\beta_{B^+}}{\beta_{H^+}} = \rho_{B^+}(\infty) 10^{\text{pH} - \text{pK}_{H^+} + \text{pK}_{B^+}} \quad (30)$$

where we have defined pH of the bulk as $\text{pH} = -\log_{10} [\rho_{H^+}(\infty)]$ and $Z_+ = |Z_{H^+}| = |Z_{B^+}|$ is the valency of counterions ($= 1$ for the monovalent ions considered in this work). $\rho_{B^+}(\infty)$ is the concentration of the cations coming from the added salt in the bulk.

Eqs. 29 and 30 capture the physics of competitive counterion adsorption on the polyelectrolyte chains in the limit of vanishing monomer density. Eqs. 15 and 16 capture the same in an inhomogeneous medium at finite monomer density. In the next section, we'll demonstrate that $\beta^*(\mathbf{r})$, which determines the charge regulation in polyelectrolyte brushes, is highly sensitive to the competitive counterion adsorption captured by Eqs. 29 and 30. In the particular case, when the counterions from the added salt don't adsorb on the polyelectrolyte chains, $\text{pK}_{B^+} \rightarrow -\infty$ and $\beta_{B^+} \rightarrow 0$ and $\beta_{H^+} = 1/\left[1 + 10^{\text{pH}-\text{pK}_{H^+}} e^{-Z_+\psi^*(\infty)/2.303}\right]$. For this case, the degree of adsorption of the counterions from the salt ($\beta_{B^+} = 0$) and protons (β_{H^+}) become independent of the bulk salt concentration. However, in general, β_{H^+} decreases and β_{B^+} increases with an increase in the bulk salt concentration. Furthermore, in general, the dipoles formed as a result of the adsorption of counterions from the salt have higher moments in comparison to those formed by the adsorption of protons. In the next section, this difference in the dipole moments is shown to play an important role in affecting the dielectric function within a polyelectrolyte brush.

Similarly, the chemical potential of solvent molecules is given by

$$\mu_s = \frac{w_{ss}\rho_{so}}{2} - \ln 4\pi + \ln \left[\frac{n_s}{\int d\mathbf{r} \exp[-w_s^*(\mathbf{r})]} \right] = \frac{w_{ss}\rho_{so}}{2} - \ln 4\pi + \ln \rho_{so} + w_s^*(\infty). \quad (31)$$

Taking the homogeneous bulk solution as the reference frame, we can write the free energy at the saddle-point as $F^* = F_{ref}^* + \Delta F^*$, where $F_{ref}^* = \sum_{\gamma=H^+, B^+, A^-, s} \mu_\gamma n_\gamma$. In this work, we are interested in the effect of inhomogeneities on the properties of polyelectrolyte brushes and ΔF^* is the contribution to the free energy arising from the inhomogeneous distributions of fields. Because the free energy is defined with in an arbitrary constant, we subtract a constant to ensure that $\Delta F^* = 0$ in the absence of inhomogeneities. Explicitly, ΔF^* is given by

$$\Delta F^* = F_{self} + F_{chemical} + F_w + F_{ions} + F_{solvent} + F_e + F_{poly}, \quad (32)$$

where $F_{self}/k_B T = [w_{pp}\rho_{po}/2 - \ln 4\pi]nN$ and

$$\begin{aligned} F_{chemical} = & nN [\beta_{B^+} \ln K_{B^+} - (1 - \beta_{H^+}) \ln K_{H^+}] \\ & + nN \left[\sum_{\gamma'} \beta_{\gamma'} \ln \beta_{\gamma'} + \left(1 - \sum_{\gamma'} \beta_{\gamma'} \right) \ln \left[1 - \sum_{\gamma'} \beta_{\gamma'} \right] \right], \end{aligned} \quad (33)$$

where $\gamma' = H^+, B^+$ and

$$F_w = \chi_{ps} \int d\mathbf{r} \rho_p^*(\mathbf{r}) \rho_s^*(\mathbf{r}) \quad (34)$$

$$F_{ions} = \sum_{\gamma=H^+, B^+, A^-} \int d\mathbf{r} \left[\rho_\gamma^*(\mathbf{r}) \ln \left[\frac{\rho_\gamma^*(\mathbf{r})}{\rho_{\gamma o}} \right] - \rho_\gamma^*(\mathbf{r}) + \rho_{\gamma o} \right] \quad (35)$$

$$F_{solvent} = \int d\mathbf{r} \left[\rho_s^*(\mathbf{r}) \ln \left[\frac{\rho_s^*(\mathbf{r})}{\rho_{so}} \right] - \rho_s^*(\mathbf{r}) + \rho_{so} \right] \quad (36)$$

$$F_e = \int d\mathbf{r} \left[\sum_{\gamma=H^+, B^+, A^-} Z_\gamma \rho_\gamma^*(\mathbf{r}) \psi^*(\mathbf{r}) + \psi_p^*(\mathbf{r}) \rho_p^*(\mathbf{r}) \right] + \frac{1}{8\pi l_{Bo}} \int d\mathbf{r} \psi^*(\mathbf{r}) \nabla_{\mathbf{r}}^2 \psi^*(\mathbf{r}) \\ - \int d\mathbf{r} \rho_s^*(\mathbf{r}) \ln \left[\frac{\sinh(p_s |\nabla_{\mathbf{r}} \psi^*(\mathbf{r})|)}{(p_s |\nabla_{\mathbf{r}} \psi^*(\mathbf{r})|)} \right] \quad (37)$$

$$F_{poly} = -\sigma \int d\mathbf{r}_{2d} \ln [\bar{q}(\{\mathbf{r}_{2d}, \delta\}, N)] - i \int d\mathbf{r} \rho_p^*(\mathbf{r}) w_p^*(\mathbf{r}) \quad (38)$$

where $\rho_s^*(\mathbf{r}) = \rho_{so} [1 - \rho_p^*(\mathbf{r})/\rho_{po}]$.

D. Numerical methods

We have solved the non-linear set of equations assuming lateral homogeneity in the planar polyelectrolyte brush. For the brush in equilibrium with the solution bath, the above equations are written in dimensionless form and the direction perpendicular to the grafting plane is assigned as the z axis in Cartesian coordinates. All of the quantities having dimensions of length are made dimensionless by dividing them by $R_{go} = (Nl^2/6)^{1/2}$. Numerical calculations ensuring that the electric field far from the brush region approaches zero, demand a box length as high as $100R_{go}$, especially in low salt conditions such as 1 millimolar (mM). For the highest bulk salt concentration of 100 mM, a box length of $20R_{go}$ is found to be sufficient. However, the monomer density decays to zero within a distance of $10-15R_{go}$ from the grafting surface for all the cases investigated in this work. Numerical results presented in this work have been obtained by taking the maximum box length of $100R_{go}$ with 512 grid points.

The modified diffusion equation represented by Eq. 22 and the Poisson-Boltzmann equation (Eq. 12) have been solved by using implicit-explicit scheme known as the extrapolated gear method[47, 48]. In order to use the extrapolated gear method, we rewrite Eq. 12 in

the form

$$\frac{\partial \psi^*(\mathbf{r})}{\partial \bar{t}} = \nabla_{\mathbf{r}} \cdot \left[\frac{1}{l_B \{\rho_p^*, \psi^*\}} \nabla_{\mathbf{r}} \psi^*(\mathbf{r}) \right] + 4\pi \rho_e^*(\mathbf{r}) \quad (39)$$

where \bar{t} is a *fictitious* time and $\rho_e^*(\mathbf{r}) = \sum_{\gamma=H^+, B^+, A^-} Z_{\gamma} \rho_{\gamma}^*(\mathbf{r}) + Z_p \beta^*(\mathbf{r}) \rho_p^*(\mathbf{r})$ is the local charge density. The steady state solution of Eq. 39 is Eq. 12. Before implementing the extrapolated gear method in one dimension, we rewrite Eq. 39 as

$$\frac{\partial \psi^*(z)}{\partial \bar{t}} = \frac{\lambda_{max}}{2} \frac{\partial^2 \psi^*(z)}{\partial z^2} + \frac{\partial}{\partial z} \left[\left[\frac{1}{l_B \{\rho_p^*, \psi^*\}} - \frac{\lambda_{max}}{2} \right] \frac{\partial \psi^*(z)}{\partial z} \right] + 4\pi \rho_e^*(z) \quad (40)$$

where $\lambda_{max} = 1/[l_B \{\rho_p^*, \psi^*\}]_{min}$ is chosen as the maximum value of inverse of the local Bjerrum length at each time step. In the extrapolated gear method, the first term on the right hand side of Eq. 40 is treated implicitly and the rest is treated explicitly. The particular choice of λ_{max} is motivated by the studies on the phase field models[48], which require the solution of similar equations. An explicit scheme is used for the initialization of the extrapolated gear method.

An equation similar to Eq. 40 is written while solving Eq. 22 with the choice $\lambda_{max} = 1/2$. Furthermore, Crank-Nicholson scheme is used to initialize the gear method for the modified diffusion equation. Dirichlet boundary conditions are used for \hat{q} and \bar{q} at the substrate i.e., $\hat{q}(z = 0, t) = \bar{q}(z = 0, t) = 0$ for all values of t . The grafted ends are displaced to the first grid point in the solution so that $\delta = 0.19R_{go}$ for a box length of $100R_{go}$ with 512 grid points. Also, steps of 10^{-4} and 10^{-3} are used for the time stepping while solving the Poisson-Boltzmann and the modified diffusion equations, respectively.

In the absence of external electric fields, we have chosen $\psi^*(\infty) = 0$. Starting from an initial guess for the fields (w_p^*, ψ^*) and charge parameters $(\beta_{H^+}, \beta_{B^+})$, we use the extrapolated gear method to compute ψ^* at the next time step, which is used as a guess in the iterative scheme. On the other hand, the guessed and the computed values for w_p^*, β_{H^+} and β_{B^+} are mixed using the simple mixing scheme[43] to develop a new guess for the next iteration. Random numbers have been used as initial guesses for the fields w_p^* and ψ^* . However, Eqs. 29 and 30 are used as initial guesses for β_{H^+} and β_{B^+} , respectively. The iterative procedure is continued until the free energy of the brush (with respect to the solution bath) doesn't change within 10^{-8} .

IV. RESULTS

Although the theory is quite general, in the following we have applied it to study a brush made of chains bearing acidic groups having $\text{pK}_{H^+} = 4.66$, which mimics poly(methacrylic acid)[49]. The motivation behind this choice is the availability of data for the stability constants[50] of monovalent salts for this system and on-going experiments. For monovalent salts such as sodium chloride (NaCl) and lithium chloride (LiCl), it is found[50, 51] that $\text{pK}_{Na^+} \simeq \text{pK}_{Li^+} = 0.28$. Furthermore, we present the results for $p_{H^+} = 0.035\text{nm} \equiv 1.7$ Debye and $p_s = 0.1003\text{nm} \equiv 4.8$ Debye mimicking weakly acidic groups such as methacrylic acid[44] and water, respectively, at the room temperature. The temperature is fixed in the calculations by the choice of $l_{Bo} = 56\text{nm}$, which corresponds to room temperature. The choice of $p_s = 0.1003$ nm is motivated by the fact that the dielectric constant of water is 80 at room temperature. Note that the value of p_s chosen for the numerical work here is little higher than the actual dipole moment of water ($= 1.85$ Debye in the gas phase[44]). The origin of this lies in the neglect of hydrogen bonding and induced dipole moment effects in the theory. Overcoming this limitation of the theory is an interesting direction for future research. Also, we have taken $l = 0.3103$ nm, which corresponds to $\rho_{so} = \rho_{po} = 1/l^3 \equiv 1\text{g/cm}^3$ i.e., the density of water at room temperature. Note that the choice of $l = 0.3103$ nm is also close to the Kuhn segment length[53] of poly(methacrylic acid). We have solved the equations at the saddle-point in three dimensional space for $N = 100$ and our preliminary studies show that a grafting density of $\sigma R_{go}^2 = 1$ for $\chi_{ps}l^3 = 0.6$ is high enough to ensure that there are no lateral inhomogeneities. Note that the choice of $\chi_{ps}l^3 = 0.6$ represents a slightly poor-solvent quality for the polyelectrolyte chain backbone, which is definitely the case for poly(methacrylic acid) in an aqueous medium. All the results presented below are for $N = 100$ and $\chi_{ps}l^3 = 0.6$.

Using these set of parameters relevant for poly(methacrylic acid) in an aqueous medium, we have varied the salt concentration and the pH of the bulk solution. To study the effect of adsorption of counterions coming from the salt, we have considered two cases. The first corresponds to $\text{pK}_{B^+} = 0.28$ and the second corresponds to $\text{pK}_{B^+} \rightarrow -\infty$, which represents the scenario in which the counterions from the salt do not adsorb on the chains. For the first case, where counterions from the salt can also adsorb on the acidic chains, we have taken $p_{B^+} = 0.125$ nm (corresponding to dipole moment of 6 Debye for the sodium carboxylate

(-COONa) group[52]).

A. Effects of the bulk salt concentration

1. Monomer density profiles, charge regulation and the dielectric function

In Fig. 2 we present the results obtained for the polyacidic brushes when the bulk salt concentration, $c_s = \rho_{B^+}(\infty)$, is varied. These results correspond to bulk pH = 5 and $\text{pK}_{B^+} \rightarrow -\infty$ so that counterions coming from the salt don't adsorb on the chains.

Monomer density profiles (Fig. 2(a)) show a depletion zone near the substrate, which is an outcome of using Dirichlet boundary conditions for the chain propagator at the substrate and a delta function as the initial condition. These boundary conditions correspond to a non-adsorbing and highly repulsive substrate. Also, the monomer density profiles approach zero around $z/R_{go} = 6 - 10$, depending on the bulk salt concentration. Furthermore, the maxima in the monomer density profiles decreases in magnitude with an increase in the bulk salt concentration. In other words, the height of the brush as manifest in the total extent of the chains increases with an increase in the bulk salt concentration. This is an outcome of an increase in the local charge inside the brush as the bulk salt concentration increases, which is reflected in Fig. 2(c).

The monomer density profiles affect the dielectric function in a significant manner as shown in Fig. 2(b). First, it is worth noting that the dielectric function closely follows the monomer density and a dielectric decrement is observed inside the brush region. The dielectric decrement is an outcome of the fact that the acidic groups on the chains are less polar than the solvent ($p_{H^+} < p_s$). The actual magnitude of the local dielectric function depends on the local density, electric field, temperature and the dipole moment of ion-pairs. In this work, we have fixed the temperature at room temperature by choosing $l_{Bo} = 56$ nm. In the region far from the grafting plane where the monomer density is zero, a dielectric constant of 80 is obtained, representing solvent rich areas. Inside the brush, the dielectric decrement is as high as 30, and it is seen that the dielectric decrement decreases with an increase in the bulk salt concentration. The decrease in the dielectric decrement is a result of a decrease in the local monomer density due to an increase in the local charge, as shown in Fig. 2(c).

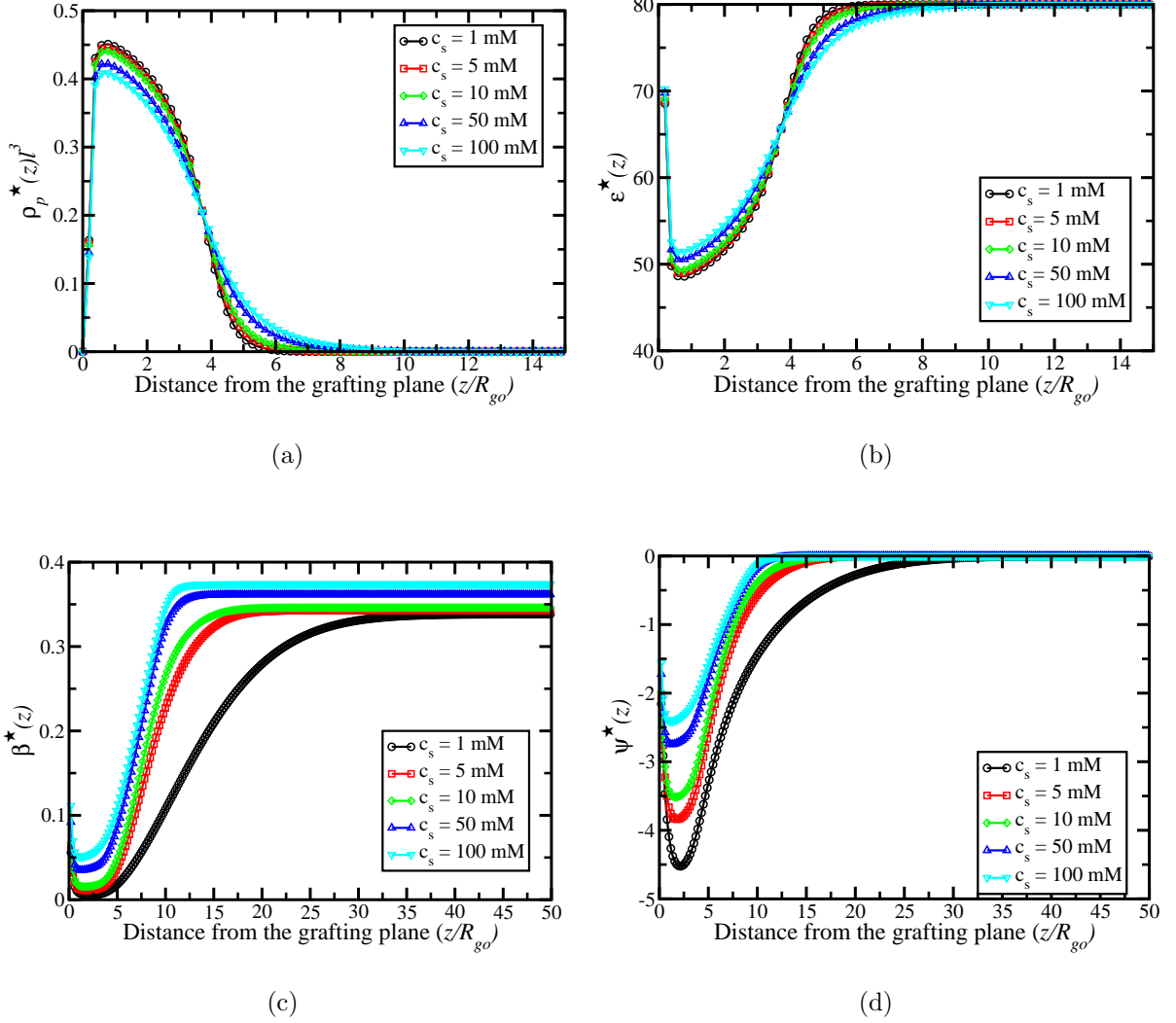


FIG. 2: Effect of the bulk salt concentrations on properties of the polyacidic brush in the case where counterions from the salt don't adsorb on the chains. These results are obtained for bulk $\text{pH} = 5$ and $\text{pK}_{B^+} \rightarrow -\infty$. Other parameters are presented in the main text. Figs. (a),(b),(c) and (d) correspond to the monomer density ($\rho_p^*(z)$), local dielectric function ($\epsilon^*(z)$), probability of finding a monomer in a charged state ($\beta^*(z)$) and the electrostatic potential ($\psi^*(z)$), respectively. The saddle-point equations are solved for $z_{max}/R_{go} = 100$ and the data is cut at $z/R_{go} = 15$ and 50 to highlight the important features for the Figs. (a)-(b) and (c)-(d), respectively.

From Fig. 2 (c) it is found that the probability of finding a monomer in the charged state ($\beta^*(z)$) is higher in the bulk solution and decreases inside the brush region followed by an increase in the depletion zone near the substrate. This is in agreement with the fact that the degree of ionization of polyelectrolytes decreases with an increase in monomer density[41].

Also, comparing the results from the calculations for different bulk salt concentrations, it is clear that the magnitude of $\beta^*(z)$ increases with an increase in the bulk salt concentration. In other words, extent of charging of the polyelectrolyte chains increases with an increase in the bulk salt concentrations. This is a result of the decrease in the electrostatic potential with an increase in the bulk salt concentration (Fig. 2 (d)), which leads to a shift in pK_{H^+} (Eq. 20). Similar effects of the salt concentration on the charge regulation are observed in recent theoretical calculations[16] and experiments[40].

The non-monotonic behavior of the probability of finding a monomer in the charged state is closely related to the non-monotonic behavior of the electrostatic potential as shown in Fig. 2 (d). It is observed that the electrostatic potential is negative everywhere for the polyacidic brush and approaches zero as far as $z/R_{go} = 50$ for the cases where the monomer density approaches zero at $z/R_{go} \sim 6 - 10$ (cf. Fig. 2 (a)). This long-range behavior of the electrostatic potential complicates the numerical investigation of the strongly charged polyelectrolyte brushes in the absence of salt. We haven't extended the study to salt-free strongly charged polyelectrolyte brushes precisely because of this reason. However, we expect the results to be qualitatively similar.

Inside the brush region (i.e., $z/R_{go} < 6 - 10$ depending on the bulk salt concentration), the electrostatic potential closely follows the monomer density profiles (compare Figs. 2 (a) and 2 (d)). The minima in the electrostatic potential corresponds to the maxima in the monomer density profiles and inside the depletion zone, the magnitude of the electrostatic potential decreases due to a decrease in the monomer number density. An increase in the bulk salt concentration leads to an increase in the local degree of charging ($\beta^*(z)$) and the electrostatic potential also increases in magnitude, as seen in Fig. 2 (d).

2. Counterion and coion distribution

Figs. 3(a) and 3(b) show the density profiles for the “free” counterions (i.e., positively charged H^+ and B^+ ions) and coions (i.e., negatively charged A^- ions), respectively, for different concentrations of the salt as set by the bulk solution. Physically, electrostatic attraction between the charged monomers and the counterions are responsible for an increase in the density of the counterions inside the brush region in comparison with the bulk. Similarly, electrostatic repulsion between the charged monomers and co-ions are the reason

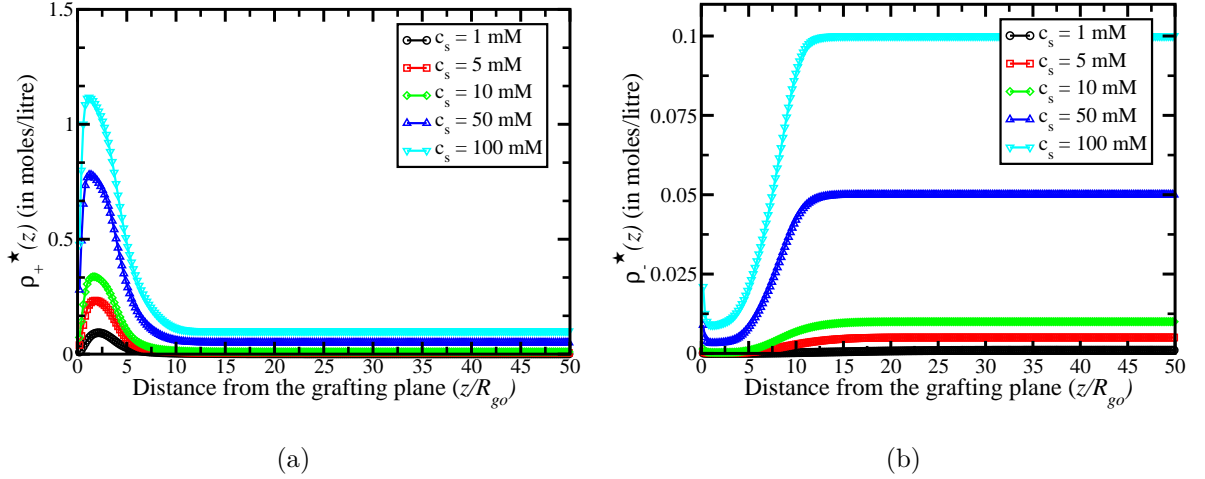


FIG. 3: Distributions of small ions at pH = 5 and different salt concentrations in the case where counterions from the salt don't bind on to the chains. Figs. (a) and (b) show the total counterion and co-ion density profiles, respectively. The parameters used for producing these figures are the same as in Fig. 2 and the data is cut at $z/R_{go} = 50$.

behind a lower number density of co-ions inside the brush region compared to the bulk solution as shown in Fig. 3(b).

The magnitudes of the electrostatic attraction and repulsion for the monomer-counterion and monomer-co-ion pairs, respectively, are related to the electrostatic potential profiles shown in Fig. 2(d). The non-monotonic behavior of the electrostatic potential manifests in the counterion and co-ion density profiles. Furthermore, the strength of these interactions is modulated by a change in the bulk salt concentration. For example, an increase in the bulk salt concentration leads to an increase in the degree of charging of monomers ($\beta^*(z)$) and electrostatic potential ($\psi^*(z)$), and increases the effect of electrostatic attractions and repulsions, as seen in Fig. 3.

At this point, we comment on an important issue not considered in this work. We note that non-trivial effects such as the partitioning of small ions based on the ion solvation energy are not taken into account. However, we can infer the effects of solvation energy by the fact that solvation energy of small ions (within Born's theory[44]) is inversely proportional to the dielectric constant. This, in turn, means that the ions prefer regions of higher dielectric functions over regions of low dielectric functions. In the case of the co-ions inside a polyelectrolyte brush showing dielectric decrement, this effect works in synergy with

the electrostatic repulsion between the monomers and the ions. In contrast, in the case of the counterions, the solvation effect counteracts the electrostatic attraction between the monomers and the coions. Depending on the relative strength of these counteracting effects, the counterion density may show a non-monotonic behavior when the solvation effects are taken into account. However, treatment of the solvation energy of charges on the chains complicates the analysis and this important direction of research is reserved for future work.

B. Effects of the competitive counterion adsorption

Fig. 4 shows different characteristics of the poly(acid) brushes for $\text{p}K_{B^+} = 0.28$ so that counterions from the added salt can also adsorb on the polyelectrolyte chains. From Figs. 2 and 4, it is found that the monomer density profiles and the dielectric function profiles are qualitatively similar in the two cases of counterion adsorption. However, there are quantitative differences and in particular, the charge regulation is affected in a significant manner as seen in Fig. 4(c). For example, with an increase in the bulk salt concentration, $\beta^*(z)$ in the bulk solution, first increases (for $c_s \leq 10$ mM) and then decreases (for $c_s = 50, 100$ mM). However, inside the brush region, $\beta^*(z)$ increases with an increase in the salt concentration, as seen in Fig. 2(c) also. The increase in the $\beta^*(z)$ with an increase in the salt concentration should be interpreted as a screening effect, which modifies the electrostatic potential (cf. Fig. 4(d)) and in turn, the extent of counterion adsorption. This effect depends on the concentration of “free” ions (see Figs. 5(a) and 5(b)). However, in the case where counterions from the salt can also adsorb, Eqs. 29 and 30, which are strictly valid at zero monomer density, reveal that an increase in the salt concentration at a fixed pH leads to the adsorption of more counterions from the salt due to enhanced dissociation of protons. This effect is observed in Fig. 4(c) for finite monomer density at $c_s = 50, 100$ mM, where the bulk value of $\beta^*(z)$ decreases with an increase in the bulk salt concentration.

In other words, an increase in the bulk salt concentrations causes the counterion adsorption equilibrium to shift toward an increase in the adsorption of the counterions from the salt at the expense of dissociation of protons. Due to the fact that ion-pairs formed due to the adsorption of counterions from the salt are more polar than the native acid groups, the dielectric function is also affected by the shift in the counterion adsorption equilibrium. This can be observed by comparing Figs. 2(b) and 4(b). For example, at $c_s = 100$ mM the

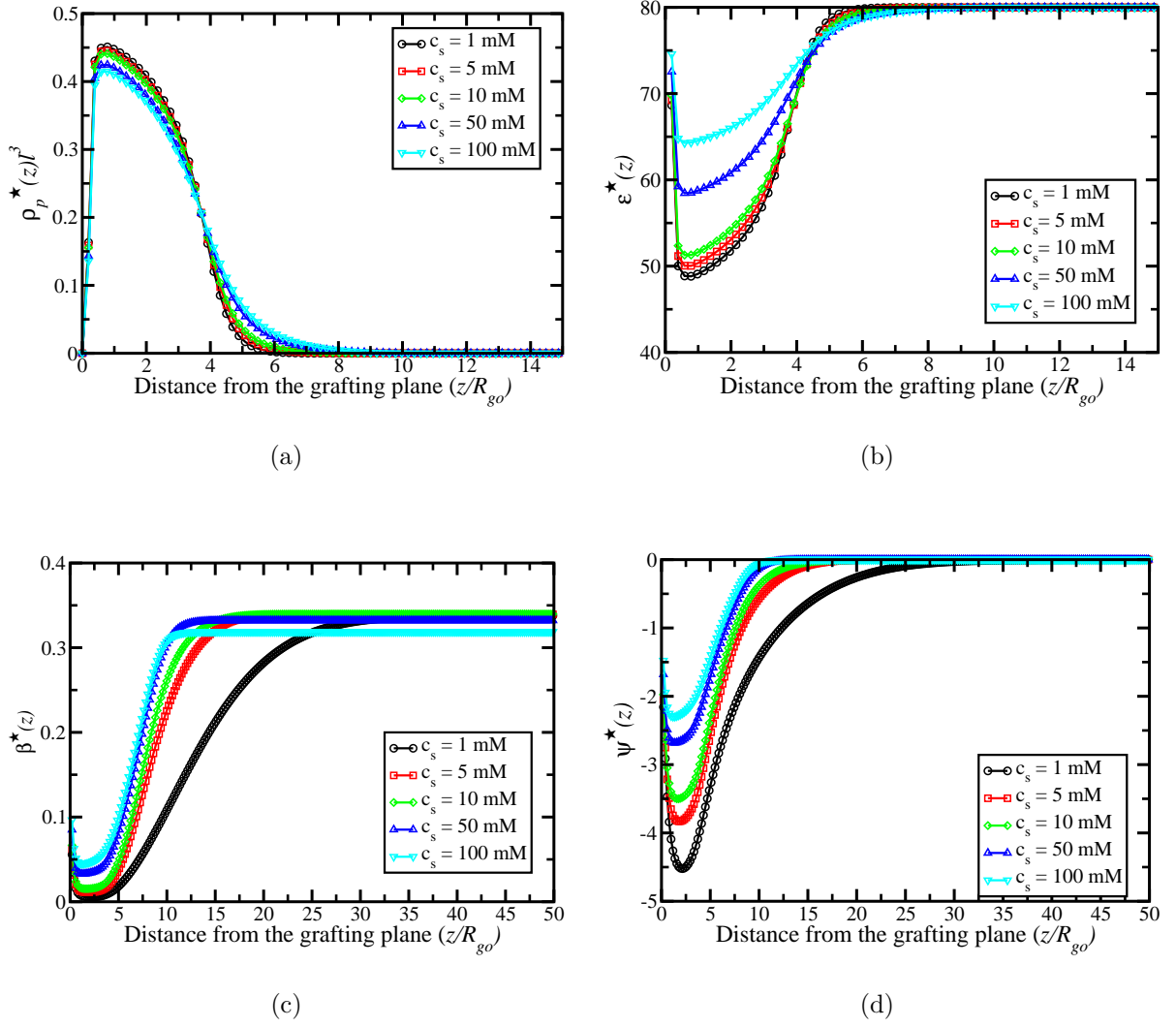


FIG. 4: Effect of the bulk salt concentrations on properties of the polyacidic brush in the case where counterions from the salt can also bind for the bulk $\text{pH} = 5$ and $\text{pK}_{B^+} = 0.28$. All the other parameters are the same as in Fig. 2. Figs. (a),(b),(c) and (d) correspond to the monomer density ($\rho_p^*(z)$), local dielectric function ($\epsilon^*(z)$), probability of finding a monomer in a charged state ($\beta^*(z)$) and the electrostatic potential ($\psi^*(z)$), respectively. Like Fig. 2, the data is cut at $z/R_{go} = 15$ and 50 to highlight the important features for the Figs. (a)-(b) and (c)-(d), respectively.

lowest local dielectric function inside the brush is ~ 65 for $\text{pK}_{B^+} = 0.28$ in comparison to the value of ~ 50 for $\text{pK}_{B^+} \rightarrow -\infty$. In the next section, we demonstrate that the shift in the counterion adsorption equilibrium from protons toward salt ions can also lead to dielectric increment just by modulating pH of the bulk solution.

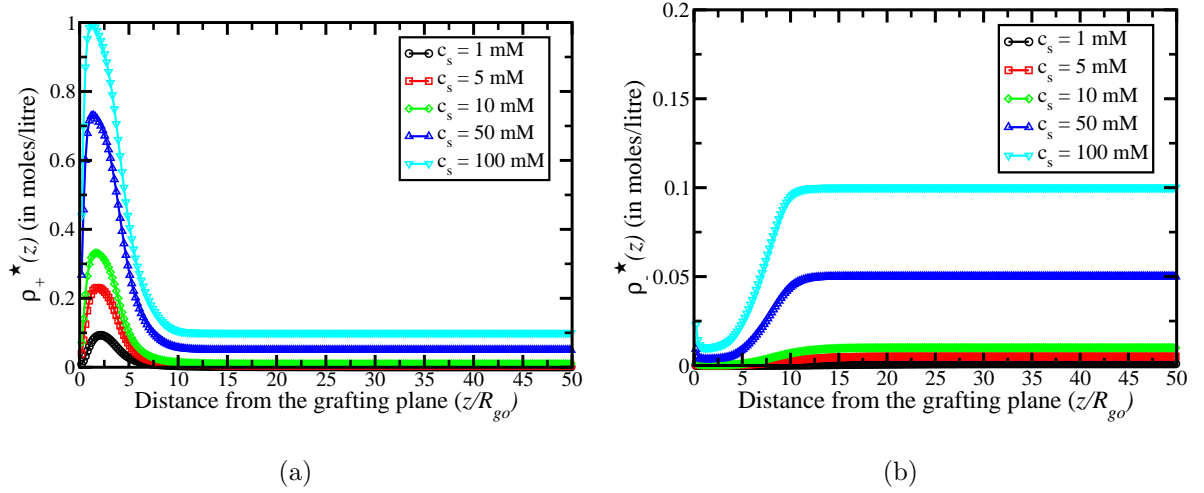


FIG. 5: Distributions of the counterions (a) and co-ions (b) for $\text{pH} = 5$, $\text{pK}_{B+} = 0.28$ and different salt concentrations in the bulk. Monomer densities and other properties of these brushes are shown in Fig. 4.

C. Effects of the pH of the bulk solution

It is well-known that an increase in pH of the bulk solution leads to an increase in the charge on poly(acid) chains. This, in turn, means that there are more sites for the adsorption of counterions from the salt. In Fig. 6, we present the results of calculations where dielectric increment is observed due to the replacement of less polar acidic groups by more polar ion-pairs.

From Figs. 6(a) and 6(c), it is clear that both the height of poly(acid) brushes and local charge increase with an increase in pH of the bulk solution. Furthermore, the electrostatic potential increases in magnitude as the bulk pH increases. However, the dielectric function inside the brush region is greater than that of the bulk for $\text{pH} = 6, 7$ in contrast to being lower for the other pH values. As mentioned earlier, this is a direct outcome of salt ion adsorption onto the chains.

An increase in the local charge with an increase in the bulk pH affects the counterion and co-ion density profiles, as shown in Fig. 7. An increase in the local charge leads to an increase in the electrostatic potential, which manifests as an increase in the counterion density profiles and as a decrease in the co-ion density profiles.

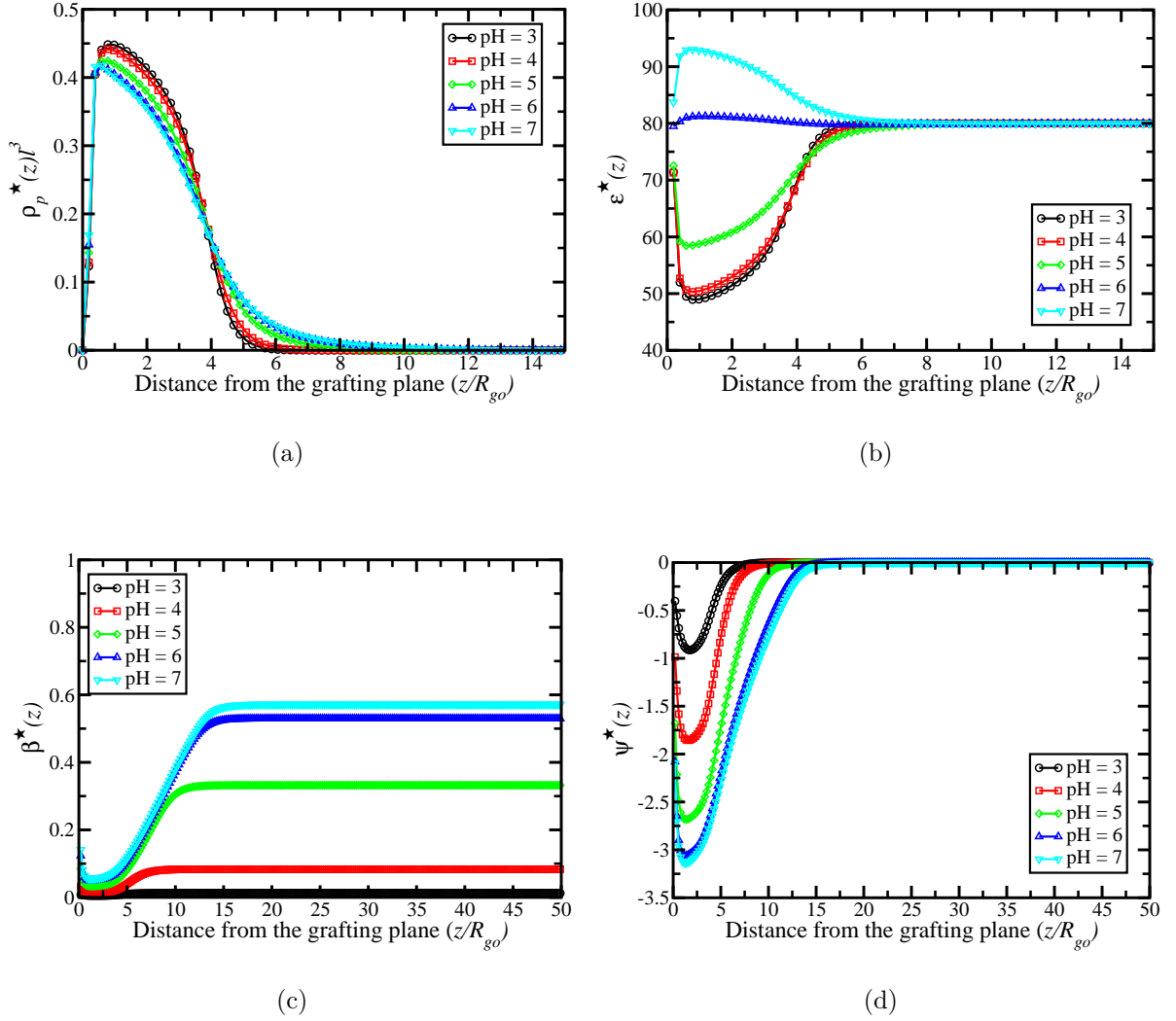


FIG. 6: Effect of the bulk pH on the properties of poly(acid) brushes at a bulk salt concentration = 50 mM and $pK_{B+} = 0.28$. All the other parameters are the same as in Fig. 2. Figs. (a),(b),(c) and (d) correspond to the monomer density ($\rho_p^*(z)$), local dielectric function ($\epsilon^*(z)$), probability of finding a monomer in a charged state ($\beta^*(z)$) and the electrostatic potential ($\psi^*(z)$), respectively. Like Fig. 2, the data is cut at $z/R_{go} = 15$ and 50 to highlight the important features for the Figs. (a)-(b) and (c)-(d), respectively.

D. Importance of non-linear effects

To highlight the importance of non-linear effects such as the dependence of the dielectric function on the local field and charge, we have compared our results with two approaches based on the assumption that the weak-coupling limit is valid independent of the coupling

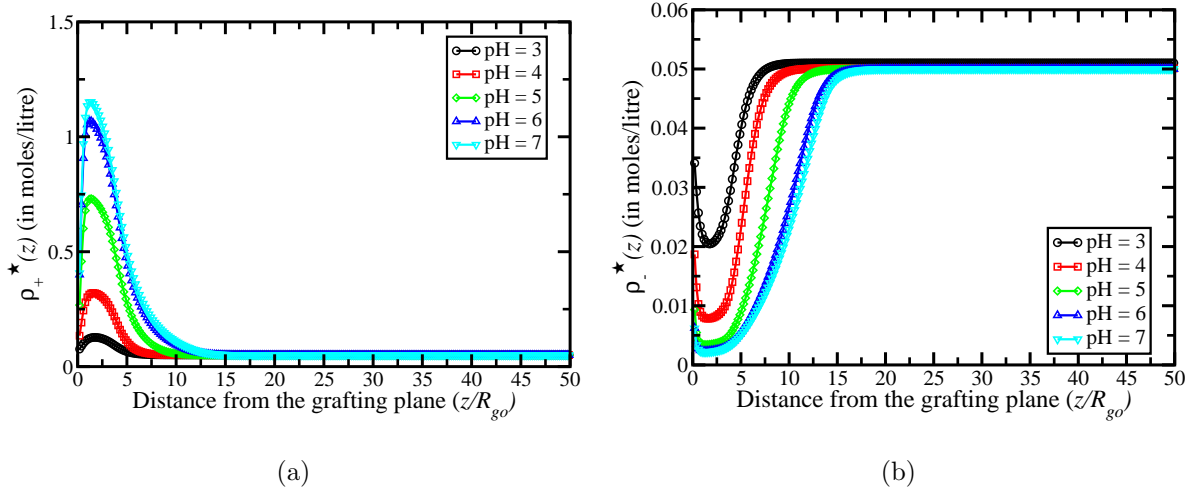


FIG. 7: Ion distributions for different pH values in the bulk at a salt concentration = 50 mM in the case where counterions from the salt also bind ($pK_{B+} = 0.28$). Figs. (a) and (b) represents the counterion and co-ion density profiles, respectively.

strength, determined by $p_{\gamma'} |\nabla_{\mathbf{r}} \psi^*(\mathbf{r})|$. In particular, we have compared (Fig. 8) the dielectric function predicted using the non-linear theory described herein with the behaviors expected from linear mixing rule for the dielectric function, which is shown to be valid in the weak coupling limit (cf. Eq. 19). Also, to highlight the importance of non-linear effects on the charge regulation and, in turn, on the dielectric function, we have compared the results obtained by calculating β_{H+} and β_{B+} using either Eq. 20 (from the full non-linear theory) or Eqs. 29 - 30, strictly valid in the limit of zero monomer density. These two approaches for the computation of dielectric function based on different estimates for β_{H+} and β_{B+} in the weak coupling limit are termed as WCLC (weak coupling limit with charge regulation) and WCLD (weak coupling limit in dilute regime), respectively. Note that the computations of the dielectric function in the WCLC and WCLD methods are done *after* solving the SCFT equations for the full non-linear theory. In case, the non-linear effects are insignificant, the results obtained from the three methods (i.e., WCLC, WCLD and the full non-linear theory) should be identical.

As seen from Fig. 8, it is clear that the non-linear effects are not important when the degree of dissociation is low such as when pH= 3 (cf. Figs. 8(a) and 6(c)), as expected. In this case, non-linear effects on the charge regulation and, in turn, on the dielectric function are insignificant. In contrast, at a moderate degree of dissociation (e.g., for pH = 5 in

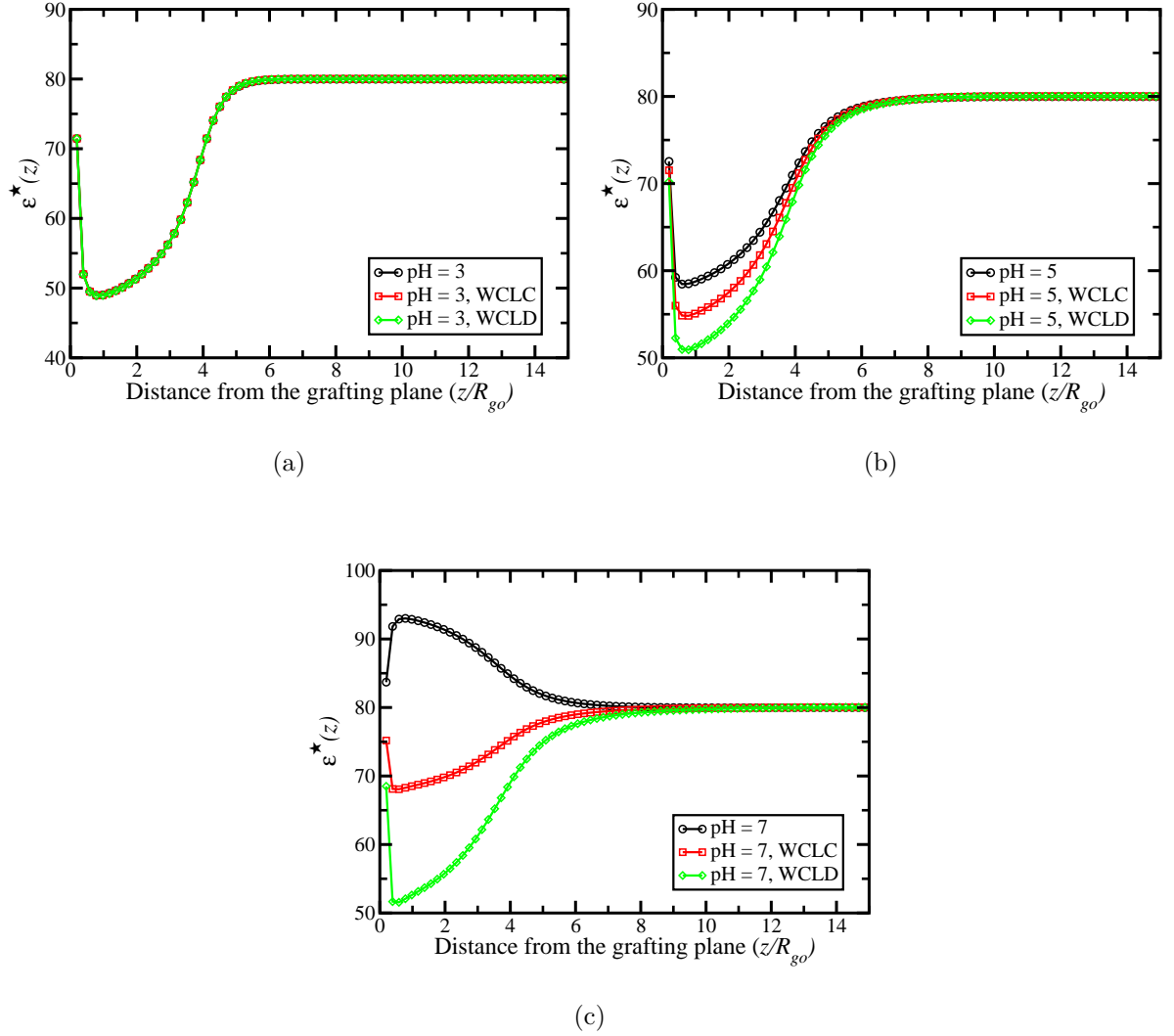


FIG. 8: Significance of the non-linear effects on the dielectric function is demonstrated here. WCLC and WCLD represent two different ways of computing the dielectric function in the weak coupling limit. For the details, see the main text. The other plots for different pH values are the same as in Fig. 6(b).

Fig. 8(b)), there are noticeable differences between the dielectric functions predicted by the different approaches. In particular, comparing the dielectric functions obtained from the WCLC and WCLD methods in Fig. 8(b), it is evident that the non-linear effects on charge regulation (arising from finite monomer density, cf. Eq. 20) play an important role. Furthermore, additional contributions arising from non-linear dependence of the dielectric function on the local field also play a significant role. These effects lead to a maximum difference of ~ 5 in the dielectric function, as seen in Fig. 8(b). The non-linear effects are

the most significant in cases where the charged groups are fully dissociated such as when the brush is in a solution at $\text{pH} = 7$, which is shown in Fig. 8(c). In this case, the non-linear theory predicts a dielectric increment inside the brush, which is in striking contrast to the dielectric decrement predicted by the WCLC and WCLD methods. The origin of this discrepancy lies in the neglect of the dependence of local dipolar density ($p_{\gamma'}^*(z)$) on the local field in the WCLC and WCLD methods. The dipolar density increases with an increase in the coupling strength ($p_{\gamma'}|\nabla_{\mathbf{r}}\psi^*(\mathbf{r})|$) as seen from Eq. 16. However, the non-linear effects are not significant far from the brush regime where $p_{\gamma'}|\nabla_{\mathbf{r}}\psi^*(\mathbf{r})| \rightarrow 0$ and the results obtained using the three different methods are the same, as expected.

V. CONCLUSIONS

We have studied planar polyelectrolyte brushes (made of end-tethered poly(acid) chains) in equilibrium with an electrolyte solution using field theory. We have focused on the quantitative description of the charge regulation and local dielectric function. Although the theory is quite general, in this work we have studied the effects of salt concentration and pH of the bulk assuming a laterally homogeneous brush. In addition, the effects of competitive counterion adsorption are studied by allowing the salt ions to form ion-pairs by adsorption onto the charged monomers.

The dipole moment of the ion-pairs is shown to significantly affect the dielectric function. For the poly(acid) chains bearing groups less polar than the solvent, the dielectric function inside the brush region is predicted to be lower than the bulk solution in the absence of adsorption of any salt ions. However, the formation of ion-pairs, generally, more polar than the solvent molecules, is shown to increase the dielectric function inside the brush in comparison to the bulk solution. Comparison of the theory taking into account dependence of the dielectric function on the local field and charge regulation (non-linear effects) with other approaches treating dielectric function by the linear mixing rules reveals that the non-linear effects are significant and must be taken into account in order to predict qualitatively correct behavior (such as the dielectric increment inside the brush) in charged systems. Furthermore, it is shown that local charge inside the brush region shows non-monotonic behavior. The local charge inside the brush region increases with an increase in the bulk salt concentration. However, the counterion adsorption equilibrium shifts from protons to

the salt ions with an increase in the salt concentration. Counterion and co-ion densities are predicted to be higher and lower, respectively, in comparison with their bulk value.

We also comment on an important assumption used in the theory. We have ignored the effects of “induced” dipole moments, which have been shown to enhance net dipole moment[29]. Ignoring this induction effect is a reasonable first step before developing a more comprehensive theory to treat the dielectric response of flexible macromolecules. In the future, we plan to overcome this limitation of the theory by extending the field theoretical method developed here.

Finally, it is understood that the dielectric function has an intricate relation with the solvation[44, 54–57] of charges. Classic work by Born[44] directly relates the solubility of charged molecules into solvents of different dielectric constants and predicts the partitioning of salt ions based on their valency and radii. In the literature it has been shown that the solvation of ions can lead to non-trivial and counter-intuitive results. For example, salt induced stabilization of the ordered morphologies in the mixtures of small molecules[58–61] is shown to be an outcome of the asymmetric[56, 62, 63] solvation of the cations and anions. The theoretical treatment presented here employs the saddle-point approximation for point ions and dipoles. Thus, the theory in the current form is unable to capture effects such as asymmetric solvation of ions based on their radii. However, the theory can be extended to finite size ions by using a soft primitive model for charges[64–66]. We plan to address this issue in a future publication.

ACKNOWLEDGMENTS

This research used resources of the Oak Ridge Leadership Computing Facility at the Oak Ridge National Laboratory, which is supported by the Office of Science of the U.S. Department of Energy under Contract No. DE-AC05-00OR22725. This research was conducted at the Center for Nanophase Materials Sciences, which is sponsored at Oak Ridge National Laboratory by the Scientific User Facilities Division, Office of Basic Energy Sciences, U.S. Department of Energy. SMKII acknowledges funding from the National Science Foundation (Grant Nos. 0840249 and 1133320) which supports experimental efforts at the University of Tennessee that in part motivated this study.

APPENDIX A : Counterion adsorption, dipolar interactions and the partition function for polyelectrolyte brushes

Here we present the partition function for the polyelectrolyte brushes in the presence of polar solvent molecules and small monovalent ions. Special attention is paid to the counterion adsorption and dipolar interactions. We start from a molecular description taking into account the dipolar interactions along with other short range interactions (dispersion and van der Waals). In order to cast theory in a field theoretical language, we rewrite the partition function in a form suitable for mathematical transformations. In this work, we consider polyelectrolyte brushes made of n mono-disperse end-tethered chains, each containing N Kuhn segments.

Following Edward's work[42], we represent a polyelectrolyte chain in the brush by a continuous curve $\mathbf{R}(t)$ of length Nl , l being the Kuhn segment length and t is the arc variable representing any point on the curve lying in the range $(0, N)$. To keep track of different chains, subscript α is used so that t_α represents the contour variable along the backbone of α^{th} chain. Also, the position vector for a particular segment, t_α , is written as $\mathbf{R}_\alpha(t_\alpha)$.

In the following, subscripts p, s and γ are used to represent monomers, solvent molecules and the small ions, respectively. Three different kinds of small ions are considered here and unless specified, $\gamma = H^+, B^+$ and A^- represents protons, cations from the salt and anions, respectively, as described in the main text. In this work, we study negatively charged (or polyacidic chains) chains and specificity of the cations is taken into account to study the effects of different binding energies of the cations. For the treatment shown below, we assume that *local* incompressibility condition is satisfied. Treating all the small ions as point-like, the incompressibility condition allows us to write the total volume as $\Omega = nN/\rho_{po} + n_s/\rho_{so}$ where ρ_{po} and ρ_{so} are the bulk monomer and solvent densities, respectively. Also, we use the notation $l^3 \equiv 1/\rho_{po}$ and \mathbf{r}_k represents the position vector of k^{th} small molecule like solvent molecules and small ions.

Furthermore, counterion adsorption on the polyelectrolyte chains is taken into account using a two-state model. Segments along the chains can be either in charged or in uncharged state. To describe the two states, another arc length variable, $\theta_\alpha(t_\alpha)$, is introduced, which enumerates the state of charging of the segment, t_α on α^{th} chain. For the analysis here,

$\theta_\alpha(t_\alpha) = 0$ means t_α is a neutral site and $\theta_\alpha(t_\alpha) = 1$ represents a fully charged site along the backbone. Like the average over all of the possible conformations in the theories of neutral polymers, we need to average over all of the possible charge distributions along the chains. We represent the average over $\theta_\alpha(t_\alpha)$ by symbol $\sum_{\{\theta_\alpha\}} \langle (\cdots) \rangle$, which explicitly means

$$\sum_{\{\theta_\alpha\}} \langle (\cdots) \rangle = \int_0^N \prod_{\alpha=1}^n dt_\alpha \int D[\theta_\alpha(t_\alpha)] (\cdots) P[\theta_\alpha(t_\alpha)] \Upsilon[\theta_\alpha(t_\alpha)]. \quad (\text{A-1})$$

Here, $P[\theta_\alpha]$ is the probability distribution function for the variable θ_α , which must satisfy the relation $\int D[\theta_\alpha(t_\alpha)] P[\theta_\alpha(t_\alpha)] = 1$. Also, $\Upsilon[\theta_\alpha(t_\alpha)]$ is the number of indistinguishable ways in which θ_α can be distributed among nN sites for a fixed number of charged sites. $\Upsilon[\theta_\alpha(t_\alpha)]$ takes into account the entropy of distribution of charged sites.

Like the segments, the counterions are also divided into two sets. One set of counterions is “free” to explore the whole space and has translational degrees of freedom. The other set is “adsorbed” on the backbone (ion-pairs) and behave as electric dipoles. Number of counterions in “free” and “adsorbed” states are taken to be n_γ^f and n_γ^a , respectively, for $\gamma = H^+, B^+$. In this work, we treat the ion-pairs as *point* electric dipoles for the development of an understanding of dielectric function. In the following, the dipole moment along the α^{th} chain backbone is written as by vector, $\mathbf{p}_\alpha(t_\alpha)$. Similarly, \mathbf{p}_k represents the dipole moment of the k^{th} solvent molecule.

Using the notations described above, the partition function (Z) for a polyelectrolyte brush can be written as

$$\begin{aligned} Z = & \int \prod_{\alpha=1}^n D[\mathbf{R}_\alpha] \sum_{\{\theta_\alpha(t_\alpha)\}} \left\langle \int \prod_{\alpha=1}^n \prod_{t_\alpha=0}^N d\mathbf{p}_\alpha(t_\alpha) \int \frac{1}{\prod_{\gamma'} n_{\gamma'}^f! n_{A^-}! n_s!} \prod_{j=1}^{n_{\gamma'}+n_s+n_{A^-}} d\mathbf{r}_j \int \prod_{k=1}^{n_s} d\mathbf{p}_k \right. \\ & \exp[-H_0\{\mathbf{R}_\alpha\} - H_w\{\mathbf{R}_\alpha, \mathbf{R}_{\alpha'}\} - H_{cp}\{\mathbf{R}_\alpha, \mathbf{p}_\alpha, \mathbf{r}_j\} - H_{pp}\{\mathbf{R}_\alpha, \mathbf{p}_\alpha, \mathbf{R}_{\alpha'}, \mathbf{p}_{\alpha'}\} \\ & \left. - H_{cc}\{\mathbf{r}_j, \mathbf{r}'_j\} - E\{\theta_\alpha\}] \prod_{\mathbf{r}} \delta\left[\frac{\hat{\rho}_p(\mathbf{r})}{\rho_{po}} + \frac{\hat{\rho}_s(\mathbf{r})}{\rho_{so}} - 1\right] \right\rangle \end{aligned} \quad (\text{A-2})$$

where $\gamma' = H^+, B^+$.

The Hamiltonian in Eq. A-2 is written by taking into account the contributions coming from the chain connectivity (given by H_0 in Eq. A-3 below), the short ranged dispersion interactions (represented by H_w in Eq. A-4) and the long range electrostatic interactions between the charged species (written as H_{pp} , H_{cp} and H_{cc} above, which correspond to the dipole-dipole, charge-dipole and charge-charge interactions, respectively). For conve-

nience in writing, in the following we have suppressed the explicit functional dependence of H_0, H_w, H_{pp}, H_{cp} and H_{cc} .

Explicitly, contributions from the chain connectivity are given by:

$$H_0 = \frac{3}{2l^2} \sum_{\alpha=1}^n \int_0^N dt_{\alpha} \left(\frac{\partial \mathbf{R}_{\alpha}(t_{\alpha})}{\partial t_{\alpha}} \right)^2 \quad (\text{A-3})$$

which is the well-known Wiener measure for a flexible polymer chain. Furthermore, $H_w \{ \mathbf{R}_{\alpha}, \mathbf{R}_{\alpha'} \}$ takes into account the energetic contributions coming from short range dispersion interactions between segments of chains indexed as α and α' located at \mathbf{R}_{α} and $\mathbf{R}_{\alpha'}$, respectively. Following Edwards's formulation[42] for a flexible chain, we model these interactions by delta functional/point interactions, which allows us to write

$$H_w = \frac{1}{2} \int d\mathbf{r} [w_{pp} \hat{\rho}_p^2(\mathbf{r}) + w_{ss} \hat{\rho}_s^2(\mathbf{r}) + 2w_{ps} \hat{\rho}_s(\mathbf{r}) \hat{\rho}_p(\mathbf{r})] \quad (\text{A-4})$$

Here, w_{pp}, w_{ss} and w_{ps} are the well-known excluded volume parameters describing the strength of interactions between $p - p, s - s$ and $p - s$ pairs, respectively. Also, $\hat{\rho}_p(\mathbf{r})$ and $\hat{\rho}_s(\mathbf{r})$ represent the microscopic number density of the monomers and the solvent molecules, respectively, at a certain location \mathbf{r} defined as

$$\hat{\rho}_p(\mathbf{r}) = \sum_{\alpha=1}^n \int_0^N dt_{\alpha} \delta[\mathbf{r} - \mathbf{R}_{\alpha}(t_{\alpha})] \quad (\text{A-5})$$

$$\hat{\rho}_s(\mathbf{r}) = \sum_{k=1}^{n_s} \delta[\mathbf{r} - \mathbf{r}_k] \quad (\text{A-6})$$

Electrostatic contributions to the Hamiltonian arising from the dipole-dipole interactions can be written by considering *finite/real* dipoles first and then systematically approaching the limit of *point* dipoles so that the dipole length goes to zero and the charge increases keeping the dipole moment finite. For *real* dipoles, we can explicitly add the Coulomb interaction energies between the charges at the ends of dipoles on the α^{th} polyelectrolyte chain and solvent molecules. The magnitude of the charges (in units of electronic charge, e) at the end of dipoles on the chains and solvent molecules are written as Z_{pk} and Z_{sk} , respectively so that $k = \pm$ and $Z_{p+} = -Z_{p-}, Z_{s+} = -Z_{s-}$. For the dipoles located on the polyelectrolyte chains, we consider their centers to lie on the chain backbone, and the dipolar axes along the vector $\mathbf{p}_{\alpha}(t_{\alpha})$. Summing over all the dipoles, we obtain the dipole-dipole interaction energy as

$$\begin{aligned}
H_{pp} = & \frac{l_{Bo}}{2} \int d\mathbf{r} \int d\mathbf{r}' \int d\mathbf{p} \int d\mathbf{p}' \left[\left\{ \frac{Z_{p+}^2}{|\mathbf{r} - \mathbf{r}' + 0.5\mathbf{p} - 0.5\mathbf{p}'|} + \frac{Z_{p-}^2}{|\mathbf{r} - \mathbf{r}' - 0.5\mathbf{p} + 0.5\mathbf{p}'|} \right. \right. \\
& + \frac{Z_{p+}Z_{p-}}{|\mathbf{r} - \mathbf{r}' + 0.5\mathbf{p} + 0.5\mathbf{p}'|} + \frac{Z_{p+}Z_{p-}}{|\mathbf{r} - \mathbf{r}' - 0.5\mathbf{p} - 0.5\mathbf{p}'|} \left. \right\} \bar{\rho}_p(\mathbf{r}, \mathbf{p}) \bar{\rho}_p(\mathbf{r}', \mathbf{p}') \\
& + \left\{ \frac{Z_{s+}^2}{|\mathbf{r} - \mathbf{r}' + 0.5\mathbf{p} - 0.5\mathbf{p}'|} + \frac{Z_{s-}^2}{|\mathbf{r} - \mathbf{r}' - 0.5\mathbf{p} + 0.5\mathbf{p}'|} \right. \\
& + \frac{Z_{s+}Z_{s-}}{|\mathbf{r} - \mathbf{r}' + 0.5\mathbf{p} + 0.5\mathbf{p}'|} + \frac{Z_{s+}Z_{s-}}{|\mathbf{r} - \mathbf{r}' - 0.5\mathbf{p} - 0.5\mathbf{p}'|} \left. \right\} \bar{\rho}_s(\mathbf{r}, \mathbf{p}) \bar{\rho}_s(\mathbf{r}', \mathbf{p}') \\
& + 2 \left\{ \frac{Z_{p+}Z_{s+}}{|\mathbf{r} - \mathbf{r}' + 0.5\mathbf{p} - 0.5\mathbf{p}'|} + \frac{Z_{p-}Z_{s-}}{|\mathbf{r} - \mathbf{r}' - 0.5\mathbf{p} + 0.5\mathbf{p}'|} \right. \\
& + \frac{Z_{p+}Z_{s-}}{|\mathbf{r} - \mathbf{r}' + 0.5\mathbf{p} + 0.5\mathbf{p}'|} + \frac{Z_{p-}Z_{s+}}{|\mathbf{r} - \mathbf{r}' - 0.5\mathbf{p} - 0.5\mathbf{p}'|} \left. \right\} \bar{\rho}_p(\mathbf{r}, \mathbf{p}) \bar{\rho}_s(\mathbf{r}', \mathbf{p}') \left. \right] \quad (\text{A-7})
\end{aligned}$$

where $l_{Bo} = e^2/\epsilon_o k_B T$ is the Bjerrum length in vacuum and ϵ_o is the permittivity of the vacuum. Also, $k_B T$ is the Boltzmann constant times the temperature. Also, in Eq. A-7, we have defined the microscopic number density of dipoles on the chains and solvent molecules by $\bar{\rho}_p(\mathbf{r}, \mathbf{p})$ and $\bar{\rho}_s(\mathbf{r}, \mathbf{p})$, respectively. Physically, these functions describe the number of dipoles with their centers at a certain location \mathbf{r} with dipole moments given by \mathbf{p} . Formally, these are defined as

$$\bar{\rho}_p(\mathbf{r}, \mathbf{p}) = \sum_{\alpha=1}^n \int_0^N dt_{\alpha} \delta[\mathbf{r} - \mathbf{R}_{\alpha}(t_{\alpha})] \delta[\mathbf{p} - \mathbf{p}_{\alpha}(t_{\alpha})] [1 - \theta_{\alpha}(t_{\alpha})] \quad (\text{A-8})$$

$$\bar{\rho}_s(\mathbf{r}, \mathbf{p}) = \sum_{k=1}^{n_s} \delta[\mathbf{r} - \mathbf{r}_k] \delta[\mathbf{p} - \mathbf{p}_k] \quad (\text{A-9})$$

Repeating the same arguments as above, we can write the interaction energy between the charges and the dipoles as

$$\begin{aligned}
H_{cp} = & l_{Bo} \int d\mathbf{r} \int d\mathbf{r}' \int d\mathbf{p}' \left[\sum_{\gamma} Z_{\gamma} \hat{\rho}_{\gamma}(\mathbf{r}) + Z_p \hat{\rho}_{pe}(\mathbf{r}) \right] \left[\frac{Z_{p+} \bar{\rho}_p(\mathbf{r}', \mathbf{p}')}{|\mathbf{r} - \mathbf{r}' - 0.5\mathbf{p}'|} \right. \\
& + \frac{Z_{p-} \bar{\rho}_p(\mathbf{r}', \mathbf{p}')}{|\mathbf{r} - \mathbf{r}' + 0.5\mathbf{p}'|} + \frac{Z_{s+} \bar{\rho}_s(\mathbf{r}', \mathbf{p}')}{|\mathbf{r} - \mathbf{r}' - 0.5\mathbf{p}'|} + \frac{Z_{s-} \bar{\rho}_s(\mathbf{r}', \mathbf{p}')}{|\mathbf{r} - \mathbf{r}' + 0.5\mathbf{p}'|} \left. \right] \quad (\text{A-10})
\end{aligned}$$

where $\hat{\rho}_{\gamma}(\mathbf{r})$ represents the local microscopic densities for the point-like ions of type γ at \mathbf{r} , defined as

$$\hat{\rho}_{\gamma}(\mathbf{r}) = \sum_{j=1}^{n_{\gamma}} \delta[\mathbf{r} - \mathbf{r}_j] \quad \text{for } \gamma = H^+, B^+, A^-. \quad (\text{A-11})$$

Furthermore, $\hat{\rho}_{pe}(\mathbf{r})$ is the contribution to the charge density coming from the polyelectrolyte chains, given by

$$\hat{\rho}_{pe}(\mathbf{r}) = \sum_{\alpha=1}^n \int_0^N dt_{\alpha} \delta[\mathbf{r} - \mathbf{R}_{\alpha}(t_{\alpha})] \theta_{\alpha}(t_{\alpha}) \quad (\text{A-12})$$

Electrostatic interaction energy among the small ions can be written using Coulomb's law as

$$H_{cc} = \frac{l_{Bo}}{2} \int d\mathbf{r} \int d\mathbf{r}' \frac{[\sum_{\gamma} Z_{\gamma} \hat{\rho}_{\gamma}(\mathbf{r}) + Z_p \hat{\rho}_{pe}(\mathbf{r})] [\sum_{\gamma} Z_{\gamma} \hat{\rho}_{\gamma}(\mathbf{r}') + Z_p \hat{\rho}_{pe}(\mathbf{r}')]}{|\mathbf{r} - \mathbf{r}'|}, \quad (\text{A-13})$$

The electrostatic terms, written for “*finite*” electric dipoles, can be written in a simplified form, if we consider the limit of “*point*” dipoles so that the length of the dipoles approaches zero. Also, as mentioned earlier, for the electric dipoles, $Z_{p+} = -Z_{p-} = Z_p$ and $Z_{s+} = -Z_{s-} = Z_s$. Approaching the limits of infinitesimal dipole lengths in such a way that the dipole moments approach their finite values, we can use multipole expansion and write

$$H_e = H_{pp} + H_{cp} + H_{cc} = \frac{l_{Bo}}{2} \int d\mathbf{r} \int d\mathbf{r}' \frac{[\hat{\rho}_e(\mathbf{r}) - \nabla_{\mathbf{r}} \cdot \hat{P}_{ave}(\mathbf{r})] [\hat{\rho}_e(\mathbf{r}') - \nabla_{\mathbf{r}'} \cdot \hat{P}_{ave}(\mathbf{r}')]}{|\mathbf{r} - \mathbf{r}'|} \quad (\text{A-14})$$

where $\hat{\rho}_e(\mathbf{r}) = \sum_{\gamma} Z_{\gamma} \hat{\rho}_{\gamma}(\mathbf{r}) + Z_p \hat{\rho}_{pe}(\mathbf{r})$ is the local charge density. Also, $\hat{P}_{ave}(\mathbf{r}') = \int d\mathbf{p} \hat{P}(\mathbf{r}, \mathbf{p}) \mathbf{p}$, is a vectorial quantity so that $\hat{P}(\mathbf{r}, \mathbf{p}) = \bar{\rho}_p(\mathbf{r}, \mathbf{p}) + \bar{\rho}_s(\mathbf{r}, \mathbf{p})$ is local dipole density at \mathbf{r} with the dipole moment \mathbf{p} . Such an expression for the electrostatic contributions resulting from polarization was proposed by Marcus[67] and Felderhof[68]. Furthermore, statistical mechanical studies have been carried out for small molecules[69–71] using this expression for the electrostatics in the free energy.

Note that the electrostatic terms written above depends on the arc length variable $\theta_{\alpha}(t_{\alpha})$. This variable also determines the energetic contributions of counterion adsorption on the backbone, written as $E\{\theta_{\alpha}\}$ in Eq. A-2. Noting that the dissociable groups on the chains have to dissociate first for the salt ions to adsorb, it is written as

$$E\{\theta_{\alpha}\} = (nN - n_{H+}^a) [\mu_{COO-}^o + \mu_{H+}^o - \mu_{COOH}^o] + n_{B+}^a [\mu_{COO-B+}^o - \mu_{COO-}^o - \mu_{B+}^o] \quad (\text{A-15})$$

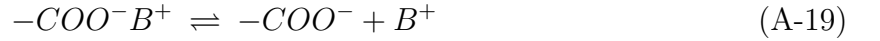
where n_{γ}^a is the number of counterions of type $\gamma' = H^+, B^+$ adsorbed on the backbone. μ_j^o is the chemical potential (in units of $k_B T$) for species of type j in infinitely dilute conditions.

The differences in the chemical potentials are related to the equilibrium constants of the corresponding reactions by the relations[45]

$$\mu_{COO^-}^o + \mu_{H^+}^o - \mu_{COOH}^o = 2.303pK_{H^+} = -2.303 \log_{10} K_{H^+} \quad (A-16)$$

$$\mu_{COO^-}^o + \mu_{B^+}^o - \mu_{COO^-B^+}^o = 2.303pK_{B^+} = -2.303 \log_{10} K_{B^+} \quad (A-17)$$

Here, we have defined K_{H^+} and K_{B^+} as the equilibrium (dissociation) constants for the reactions



respectively. Such a model of counterion adsorption was developed in the classic paper by Harris and Rice[72].

APPENDIX B : Field theory for polyelectrolyte brushes : annealed charge distribution

The probability distribution, P , needs to be determined self-consistently by the minimization of the free energy and must satisfy the relation $\int D[\theta_\alpha(t_\alpha)] P[\theta_\alpha(t_\alpha)] = 1$. In this work, we take a variational *ansatz* for P and write it as

$$P[\theta_\alpha(t_\alpha)] = \left(\sum_{\gamma'=H^+,B^+} \beta_{\gamma'} \right) \delta[\theta_\alpha(t_\alpha)] + \left(1 - \sum_{\gamma'=H^+,B^+} \beta_{\gamma'} \right) \delta[\theta_\alpha(t_\alpha) - 1] \quad (B-1)$$

so that $n_{\gamma'}^a = \beta_{\gamma'} nN$ for $\gamma' = H^+, B^+$. Mathematically, β_{H^+} and β_{B^+} are the variational parameters, which will be determined by minimization of the free energy. Physically, β_{H^+} and β_{B^+} correspond to the fraction of sites on the chains occupied by H^+ and B^+ , respectively. Furthermore, using Eq. B-1 for the charge distribution

$$\Upsilon[\theta_\alpha(t_\alpha)] = \frac{nN!}{n_{H^+}^a! n_{B^+}^a! (nN - n_{H^+}^a - n_{B^+}^a)!} \quad (B-2)$$

Such a distribution is called “annealed” distribution in the literature[73–75]. The use of Eq. B-1 for the probability distribution the charged sites on the chain backbones simplifies the subsequent analysis. Using Eq. B-1, we can write Eq. A-2 in field theoretic form. We start from the electrostatic contribution to the partition function, which is given by Eq. A-14, and use the Hubbard-Statonovich transformation[43]

$$\exp[-H_e] = \frac{1}{\Xi} \int D[\psi] \exp \left[-i \int d\mathbf{r} \left\{ \hat{\rho}_e(\mathbf{r}) - \nabla_{\mathbf{r}} \cdot \hat{P}_{ave}(\mathbf{r}) \right\} \psi(\mathbf{r}) + \frac{1}{8\pi l_{Bo}} \int d\mathbf{r} \psi(\mathbf{r}) \nabla_{\mathbf{r}}^2 \psi(\mathbf{r}) \right], \quad (\text{B-3})$$

where

$$\Xi = \int D[\psi] \exp \left[\frac{1}{8\pi l_{Bo}} \int d\mathbf{r} \psi(\mathbf{r}) \nabla_{\mathbf{r}}^2 \psi(\mathbf{r}) \right]. \quad (\text{B-4})$$

Using this transformation and Eq. B-1, we can integrate over the orientations of the dipoles analytically and evaluate the average over θ_α . Writing the magnitude of the dipole moments of solvent molecules as p_s and ion-pairs as $p_{\gamma'}$ for $\gamma' = H^+, B^+$, the partition function given by Eq. A-2 becomes

$$\begin{aligned} Z = & e^{-F_a/k_B T} \int \prod_{\alpha=1}^n D[\mathbf{R}_\alpha] \int \prod_{\gamma} \prod_{j=1}^{n_\gamma} d\mathbf{r}_j \prod_{k=1}^{n_s} d\mathbf{r}_k \frac{1}{\Xi} \int D[\psi] \exp[-H_0\{\mathbf{R}_\alpha\} - H_w\{\mathbf{R}_\alpha, \mathbf{R}_{\alpha'}\}] \\ & -i \int d\mathbf{r} \sum_{\gamma} Z_{\gamma} \hat{\rho}_{\gamma}(\mathbf{r}) \psi(\mathbf{r}) - i \int d\mathbf{r} \hat{\rho}_p(\mathbf{r}) \psi_p(\mathbf{r}) + \frac{1}{8\pi l_{Bo}} \int d\mathbf{r} \psi(\mathbf{r}) \nabla_{\mathbf{r}}^2 \psi(\mathbf{r}) \\ & + \int d\mathbf{r} \hat{\rho}_s(\mathbf{r}) \ln \left[\frac{\sin(p_s |\nabla_{\mathbf{r}} \psi(\mathbf{r})|)}{p_s |\nabla_{\mathbf{r}} \psi(\mathbf{r})|} \right] \prod_{\mathbf{r}} \delta \left[\frac{\hat{\rho}_p(\mathbf{r})}{\rho_{po}} + \frac{\hat{\rho}_s(\mathbf{r})}{\rho_{so}} - 1 \right] \end{aligned} \quad (\text{B-5})$$

where

$$\begin{aligned} \frac{F_a}{k_B T} = & n_{B^+}^a \ln K_{B^+} - (nN - n_{H^+}^a) \ln K_{H^+} - \ln \left[\frac{nN!}{n_{H^+}^a! n_{B^+}^a! (nN - n_{H^+}^a - n_{B^+}^a)!} \right] \\ & + \ln [n_{H^+}^f! n_{B^+}^f! n_s!] - (nN + n_s) \ln 4\pi \end{aligned} \quad (\text{B-6})$$

and we have absorbed numerical prefactors of 4π coming from orientational degrees of freedom of the dipoles in the definitions of K_{H^+} and K_{B^+} . Also,

$$\exp[-i\psi_p(\mathbf{r})] = (1 - \beta_{H^+} - \beta_{B^+}) \exp[-iZ_p\psi(\mathbf{r})] + \sum_{\gamma=H^+, B^+} \beta_{\gamma} \left[\frac{\sin(p_{\gamma} |\nabla_{\mathbf{r}} \psi(\mathbf{r})|)}{p_{\gamma} |\nabla_{\mathbf{r}} \psi(\mathbf{r})|} \right] \quad (\text{B-7})$$

Now, we introduce collective variables corresponding to $\hat{\rho}_p$ and $\hat{\rho}_s$ by using the identity

$$Z\{\hat{\rho}_p, \hat{\rho}_s\} = \int D[\rho_p] \int D[\rho_s] Z\{\rho_p, \rho_s\} \prod_{\mathbf{r}} \delta[\rho_p(\mathbf{r}) - \hat{\rho}_p(\mathbf{r})][\rho_s(\mathbf{r}) - \hat{\rho}_s(\mathbf{r})] \quad (\text{B-8})$$

Also, the local incompressibility constraint allows us to rewrite H_w given by Eq. A-4 in terms of collective variables as

$$H_w = \frac{1}{2} [w_{pp}\rho_{po}nN + w_{ss}\rho_{so}n_s] + \chi_{ps} \int d\mathbf{r} \rho_p(\mathbf{r}) \rho_s(\mathbf{r}), \quad (\text{B-9})$$

where we have used $\int d\mathbf{r}\hat{\rho}_p(\mathbf{r}) = nN$, $\int d\mathbf{r}\hat{\rho}_s(\mathbf{r}) = n_s$. Also, we have defined a parameter χ_{ps} by

$$\chi_{ps} = w_{ps} - \frac{w_{pp}\rho_{po}}{2\rho_{so}} - \frac{w_{ss}\rho_{so}}{2\rho_{po}} \quad (\text{B-10})$$

which has the dimensions of volume.

Now, writing the local constraints (represented by delta functions) in terms of functional integrals by the identities

$$\prod_{\mathbf{r}} \delta[\rho_j(\mathbf{r}) - \hat{\rho}_j(\mathbf{r})] = \int D[w_j] \exp \left[-i \int d\mathbf{r} w_j(\mathbf{r}) \{ \rho_j(\mathbf{r}) - \hat{\rho}_j(\mathbf{r}) \} \right] \quad \text{for } j = p, s \quad (\text{B-11})$$

and computing trivial functional integrals over $\rho_s(\mathbf{r})$, we arrive at Eq. 1. Furthermore, note that in the absence of dipolar species (i.e., $p_j = 0$ for $j = H^+, B^+, s$ in the above treatment), we recover the self-consistent field theory for “annealed” charge distributions documented in literature[74, 75].

REFERENCES

-
- [1] S. Alexander, Journal De Physique 38 (8), 983 (1977).
 - [2] P. G. Degennes, Macromolecules 13 (5), 1069 (1980).
 - [3] S. T. Milner, Science 251 (4996), 905 (1991).
 - [4] J. Ruhe, M. Ballauff, M. Biesalski, P. Dziezok, F. Grohn, D. Johannsmann, N. Houbenov, N. Hugenberg, R. Konradi, S. Minko, M. Motornov, R. R. Netz, M. Schmidt, C. Seidel, M. Stamm, T. Stephan, D. Usov, and H. N. Zhang, in Polyelectrolytes with Defined Molecular Architecture I (2004), Vol. 165, pp. 79.
 - [5] M. Ballauff and O. Borisov, Current Opinion in Colloid & Interface Science 11 (6), 316 (2006).
 - [6] M. Ballauff, Progress in Polymer Science 32 (10), 1135 (2007).
 - [7] S. Misra, S. Varanasi, and P. P. Varanasi, Macromolecules 22 (11), 4173 (1989).
 - [8] S. Misra and S. Varanasi, Journal of Chemical Physics 95 (3), 2183 (1991).
 - [9] R. S. Ross and P. Pincus, Macromolecules 25 (8), 2177 (1992).

- [10] E. B. Zhulina, T. M. Birshtein, and O. V. Borisov, *Macromolecules* 28 (5), 1491 (1995).
- [11] Y. V. Lyatskaya, F. A. M. Leermakers, G. J. Fleer, E. B. Zhulina, and T. M. Birshtein, *Macromolecules* 28 (10), 3562 (1995).
- [12] P. M. Biesheuvel, *Journal of Colloid and Interface Science* 275 (1), 97 (2004).
- [13] R. Nap, P. Gong, and I. Szleifer, *Journal of Polymer Science Part B-Polymer Physics* 44 (18), 2638 (2006).
- [14] T. Wu, P. Gong, I. Szleifer, P. Vlcek, V. Subr, and J. Genzer, *Macromolecules* 40 (24), 8756 (2007).
- [15] P. Gong, T. Wu, J. Genzer, and I. Szleifer, *Macromolecules* 40 (24), 8765 (2007).
- [16] P. Gong, J. Genzer, and I. Szleifer, *Physical Review Letters* 98 (1) (2007).
- [17] H. Seki, Y. Y. Suzuki, and H. Orland, *Journal of the Physical Society of Japan* 76 (10) (2007).
- [18] A.Y. Sankhe, S.M. Hussan, and S.M. Kilbey, *Journal of Polymer Science Part A - Polymer Chemistry* 45(4), 566 (2007).
- [19] S.B. Rahane, J.A. Floyd, A.T. Metters, and S.M. Kilbey, *Advanced Functional Materials* 18 (8), 1232 (2008).
- [20] K. N. Witte, S. Kim, and Y. Y. Won, *Journal of Physical Chemistry B* 113 (32), 11076 (2009).
- [21] M. Tagliazucchi, M. O. de la Cruz, and I. Szleifer, *Proceedings of the National Academy of Sciences of the United States of America* 107 (12), 5300 (2010).
- [22] M. J. Uline, Y. Rabin, and I. Szleifer, *Langmuir* 27 (8), 4679 (2011).
- [23] M. Mandel and A. Jenard, *Transactions of the Faraday Society* 59 (489), 2158 (1963).
- [24] M. Mandel and A. Jenard, *Transactions of the Faraday Society* 59 (489), 2170 (1963).
- [25] M. Mandel and T. Odijk, *Annual Review of Physical Chemistry* 35, 75 (1984).
- [26] F. Bordi, C. Cametti and R.H. Colby, *Journal of Physics - Condensed Matter* 16 (49), R1423 (2004).
- [27] A. Minakata, N. Imai and F. Oosawa, *Biopolymers* 11(2), 347 (1972).
- [28] P. Debye, *Polar Molecules* (The Chemical Catalog Company Inc., New York, 1929).
- [29] L. Onsager, *Journal of Chemical Physics*, 58, 1486-1493 (1936).
- [30] C.J.F. Böttcher, *Theory of Electric Polarization* (Elsevier, Amsterdam, 1973).
- [31] F. Booth, *Journal of Chemical Physics* 19 (4), 391 (1951).
- [32] F. Booth, *Journal of Chemical Physics* 23 (3), 453 (1955).
- [33] R. L. Fulton, *Journal of Chemical Physics* 130 (20), 204503 (2009).

- [34] L. Sandberg and O. Edholm, *Journal of Chemical Physics* 116 (7), 2936 (2002).
- [35] A.K. Jha and K.F. Freed, *Journal of Chemical Physics* 128 (3), 034501 (2008).
- [36] H. Gong and K.F. Freed, *Physical Review Letters* 102 (5), 057603 (2009).
- [37] G.S. Manning, *Journal of Chemical Physics* 51 (3), 924 (1969).
- [38] V.M. Prabhu, *Current Opinion in Colloid Interface Science* 10 (1-2), 2 (2005).
- [39] Y. Levin, *Reports on Progress in Physics* 65 (11), 1577 (2002).
- [40] S. Wang, S. Granick and J. Zhao, *Journal of Chemical Physics* 129 (24), 241102 (2008).
- [41] M. Muthukumar, *Journal of Chemical Physics* 120 (19), 9343; R. Kumar, A. Kundagrami and M. Muthukumar, *Macromolecules* 42 (4), 1370 (2009).
- [42] M. Doi and S.F. Edwards, *The Theory of Polymer Dynamics* (Clarendon Press, Oxford, 1986).
- [43] G.H. Fredrickson, *The Equilibrium Theory of Inhomogeneous Polymers* (Oxford University, New York, 2006).
- [44] J.N. Israelachvili, *Intermolecular and Surface Forces* (Academic Press: San Diego, CA, 1987).
- [45] D.A. McQuarrie, *Statistical Mechanics*, (University Science Books, Sausalito, CA, 2000).
- [46] M. Muller, *Physical Review E* 65 (3), 030802 (2002).
- [47] U. M. Ascher, S. J. Ruuth, and B. T. R. Wetton, *Siam Journal on Numerical Analysis* 32 (3), 797 (1995).
- [48] V. E. Badalassi, H. D. Cenicerros, and S. Banerjee, *Journal of Computational Physics* 190 (2), 371 (2003).
- [49] J. Wen in *Polymer Data Handbook* (Oxford University Press Inc., 1999).
- [50] L.G. Sillen and A.E. Martell, *Stability Constants of Metal-Ion Complexes: Suppl. 1* (Alden: Oxford, 1964).
- [51] H.P. Gregor and M. Frederick, *Journal of Polymer Science* 23 (103), 451 (1957).
- [52] K. Arai and A. Eisenberg, *Journal of Macromolecular Science, Part B: Physics* 17(4), 803 (1980).
- [53] C. Ortiz and G. Hadziioannou, *Macromolecules* 32 (3), 780 (1999).
- [54] B.W. Ninham and V. Yaminsky, *Langmuir* 13 (7), 2097 (1997).
- [55] M. Bostrom and B. W. Ninham, *J. Phys. Chem. B* 108 (33), 12593 (2004).
- [56] A. Onuki and H. Kitamura, *Journal of Chemical Physics* 121 (7), 3143 (2004).
- [57] Z. G. Wang, *Journal of Physical Chemistry B* 112 (50), 16205 (2008).
- [58] K. Sadakane, H. Seto and M. Nagao, *Chemical Physics Letters* 426 (1-3), 61 (2006).

- [59] K. Sadakane, H. Seto, H. Endo and M. Kojima, *Journal of Applied Crystallography* 40 (1), S527 (2007).
- [60] K. Sadakane, H. Seto, H. Endo and M. Shibayama, *Journal of the Physical Society of Japan* 76 (11), 113602 (2007).
- [61] K. Sadakane, A. Onuki, K. Nishida, S. Koizumi and H. Seto, *Physical Review Letters* 103 (16), 167803 (2009).
- [62] V. M. Nabutovskii, N. A. Nemov and Y. G. Peisakhovich, *Physics Letters A* 79 (1), 98 (1980).
- [63] V. M. Nabutovskii, N. A. Nemov and Y. G. Peisakhovich, *Molecular Physics* 54 (4), 979 (1985).
- [64] Z.G. Wang, *Physical Review E* 81 (2), 021501 (2010).
- [65] D. Coslovich, J. Hansen, and G. Kahl, *Journal of Chemical Physics* 134 (24), 244514 (2011).
- [66] R. Riggleman, R. Kumar, and G.H. Fredrickson, *Journal of Chemical Physics* 136 (2), 024903 (2012).
- [67] R.A. Marcus, *Journal of Chemical Physics* 24 (5), 979 (1956).
- [68] B.U. Felderhof, *Journal of Chemical Physics* 67 (2), 493 (1977).
- [69] R.D. Coalson and A. Duncan, *Journal of Physical Chemistry* 100 (7), 2612 (1996).
- [70] A. Abrashkin, D. Andelman, and H. Orland, *Physical Review Letters* 99 (7), 077801 (2007).
- [71] Z.G. Wang, *Journal of Theoretical and Computational Chemistry* 7 (3), 397 (2008).
- [72] F. E. Harris, S. A. Rice, *Journal of Physical Chemistry* 58 (9), 725 (1954).
- [73] I. Borukhov, D. Andelman, and H. Orland, *European Physical Journal B* 5 (4), 869 (1998).
- [74] A. Shi and J. Noolandi, *Macromolecular Theory and Simulations* 8 (3), 214 (1999).
- [75] Q. Wang, T. Taniguchi and G.H. Fredrickson, *Journal of Physical Chemistry B* 108 (19), 6733 (2004).